Learning of odor timing

A thesis submitted to

Indian Institute of Science Education and Research Pune in partial fulfilment of the requirements for the BS-MS Dual Degree Programme

by

Atharva Arun Dingankar

Registration Number: 20151175

Indian Institute of Science Education and Research Pune

Dr. Homi Bhabha Road,

Pashan, Pune 411008, INDIA.

March, 2020

Supervisor: Dr. Nixon Abraham

Certificate

This is to certify that this dissertation entitled "**Learning of odor timing**" towards the partial fulfilment of the BS-MS dual degree programme at the Indian Institute of Science Education and Research, Pune represents study/work carried out by Atharva Arun Dingankar at Indian Institute of Science Education and Research under the supervision of Dr. Nixon Abraham, Assistant Professor, Department of Biology, during the academic year 2019-2020.

Atharva Dingankar

Dr. Nixon M. Abraham

Declaration

I hereby declare that the matter embodied in the report entitled "**Learning of odor timing**" are the results of the work carried out by me at the, Department of Biology, during the academic year 2019-2020, Indian Institute of Science Education and Research, Pune, under the supervision Dr. Nixon Abraham and the same has not been submitted elsewhere for any other degree.

Atharva Dingankar

Dr. Nixon M. Abraham

Date: 02-04-2020

Contents

List of Tables

List of Figures

Acknowledgements

I want to thank my supervisor, Dr. Nixon Abraham for his valuable guidance and support throughout my Master's thesis. His expertise in behavioral studies and analytical methods and his knowledge of the olfactory system enabled me to progress through this project while learning necessary skills. I would also like to thank my TAC advisor, Dr. Collins Assisi for closely following my project and suggesting me appropriate modifications throughout the course of this project.

I want to thank my mentor, Anindya Bhattacharjee, for teaching, and helping me throughout the course of this study. I would like to thank Priya for teaching me the procedural aspects of training on the olfactometers. I would also like to thank Meenakshi and Shruti for their timely and crucial inputs on my project. I would like thank Sarang for his valuable inputs and his help in solving technical problems in my instrument. I would like to thank Felix, Meher, Rajdeep, Avi, and Arpan for light-hearted discussions and for making the experience of working in lab enjoyable. I would like to thank NFGFHD for providing animals for my project.

Last but not the least, I am extremely thankful to my parents and my friends who have been with me through all the ups and downs during the course of this project.

1 Abstract

Our olfactory senses are challenged to smell different odorants which vary in their physical and chemical characteristics. The odorants are often transported in turbulent plumes and depending on the source of origin, may arrive to our nose at different times. However, whether the mammalian olfactory system can extract temporal information of specific odorant from the varying olfactory environment is unknown. There has been an effort to understand if the olfactory system is capable to code odor timing. One such study in rodents using optogenetic stimulations have indicated that mice can discriminate the glomerular activations at different times (Smear et al., 2013). On the contrary, a recent study with human participants reported that humans are poor in discriminating temporal odor mixtures (Perl et al., 2020). To address if mice can discriminate odorant information arriving at different times, we developed a behavioral paradigm which, allowed us to deliver odor pulses of different durations in the background of another odorant. A series of behavioral assays were designed employing the go/no-go operant conditioning paradigm and animals were trained to detect target odorant with different temporal delays. Careful analysis of different behavioral readouts associated with the sampling and licking prove that mice can discriminate temporal delays associated with different odorants. However, mice showed slower learning pace while they were challenged to discriminate the delays associated with the same odorants and few of the animals were not able to learn this highly complex task. In conclusion, our results prove that the rodent olfactory system can discriminate the odor timings in complex olfactory environments.

2 Introduction

2.1 Olfactory system and its significance in rodent olfactory behavior

All animals regularly interact with their surroundings to acquire relevant information and perform vital functions. The natural environment where we inhabit is rich in sensory stimuli originating from variable sources. Thus, the most challenging task of sensory systems is to identify the stimulus of significance and segregate from the background. The organization of sensory systems is optimized for acquiring and relaying relevant information to cortical areas with exquisite precision. Most of the sensory systems are involved in sampling sensory information, which can be defined by multiple descriptors. Different information coding schemes are involved in encoding these incoming complex stimuli for efficient extraction of relevant data about the organism's surroundings. For example, the visual system processes information from rays of light, which varies in wavelength, intensity, and chromaticity (Jacobs et al., 2001; Mitchell et al., 2017). Sound is arranged in a two-dimensional space according to their loudness and pitch. Similarly, chemosensory system like the olfactory system samples odor plumes. Odor plumes carry odor molecules that form an olfactory image of the surroundings. Different odorant molecules form different representations based on the differences in their chemical and physical characteristics. At the periphery, sensory neurons possess multiple receptor types which empower the sensory systems to sample the incoming sensory stimuli. While processing the sensory information, different coding strategies allow animals to get a stable percept of the sensory stimulus. Therefore, with an over-arching goal of understanding the formation of sensory percept, it becomes pertinent to investigate the coding strategies animals use to encode stimulus information.

The strategies to encode sensory stimuli are largely similar across different sensory systems. The visual (Udin & Fawcett, 1988) and somatosensory (Roux et al., 2018) system show a linear correlation between the location of stimulus and its neural correlate. Thus, if two points are located side-by-side in actual space, their neural correlates will be closely found to each other in the brain. In the olfactory system too, odors are first represented in the form of a map which is rich in spatial and temporal characteristics. Such a map allows efficient representation of odor stimulus in the form of a multidimensional perceptual space. Such multidimensionality is due to the nature

of odorant molecules, which vary in their chemical nature due to the different functional groups present, chain length, the binding affinities involved in odorant-receptor interaction (Ko et al., 2010), and the physical properties of the molecules (Cenier et al., 2008). For example, the relative vapor pressure of the odorants can influence olfactory perception. Another dimensionality can be introduced when odor molecules are carried with rapidly varying air plumes and thus fluctuate in space and time.

Understanding how odor percept is formed, garnered a particular interest in researchers when Buck and Axel discovered odor receptors in 1991. Scientists employed rodents as the model system to study olfaction since then for several reasons. Rodents serve as a reliable model organism for studying the olfactory system because of its vital role in their survival. In rodents, olfactory system plays a crucial role in foraging (Howard et al., 1968), interacting with conspecifics and regulating endocrinal activities (Doty, 1986). The advancement in molecular biology techniques allowed to complete sequencing of the mouse genome, and it was found to share a high degree of similarity with humans (Mouse Genome Sequencing Consortium, 2002). Thus, genetic principles applicable in mice could be extrapolated to humans to a great extent, thus offering an excellent system to study the brain in health and disease.

2.2 Organization of the rodent olfactory system

The process of odor perception begins when air containing odor molecules are inhaled through the nostrils. As the odorant molecules travel through the nose, they reach the nasal epithelium, which is lined with Olfactory Sensory Neurons (OSNs) expressing odor receptors (ORs). In the nasal epithelium, OSNs expressing different receptors are segregated into different zones across the olfactory epithelium. Although, in a given zone, ORs of various kinds are randomly distributed (Vassar et al., 1993; Zapiec & Mombaerts, 2020). Odor molecules bind to OSNs in a combinatorial fashion wherein a single odorant molecule can bind to multiple receptors and, multiple odorant molecules can activate a single receptor. Binding of odorants initiates a signal transduction process, and the axons of OSNs relay the odor information to spherical neuropil like structures within the OB, known as glomeruli. They are arranged in the form of arrays on the surficial layer of OB (Mombaerts et al., 1996; Reviewed by Nagayama et al., 2014). All OSNs expressing the same kind of OR converge to two glomeruli; one on lateral and one on the medial side (Baker et al., 2019; Mombaerts

et al., 1996; Sato et al., 2020). As a combined outcome of the combinatorial coding scheme and principle of axonal convergence onto glomeruli, odor identities are represented as spatial maps in the glomerular layer of the olfactory bulb. The olfactory system is sensitive enough to detect odorants with concentrations as low as in the millimolar range (Firestein et al., 1993). Achieving such high sensitivity for concentration has been associated with high ligand-receptor specificity and high affinity (Eaton et al., 1995). However, OSNs can physiologically respond to a broad range of odorant molecules (implying low specificity) (Firestein & Shepherd, 1991; reviewed in Lancet, 1986). Hence, it has been proposed that the high convergence rates of OSNs onto glomeruli might serve as a mechanism to increase the sensitivity of the system for detecting odorant concentrations over a broad range (Cleland & Linster, 1999). However, olfaction is a dynamic sensory modality meant to perceive olfactory stimuli fluctuating over time. As odorants bind to ORs with low specificity and affinity, the binding pattern of odorants with ORs does not remain temporally constant. The ORs which bind to the odorants with high affinity are activated first and other ORs binding with odorant molecules at low affinity are activated in time. Thus, the glomerular activation pattern evolves with time (Spors et al., 2006; Spors & Grinvald, 2002). As a result of combinatorial coding scheme and the temporal pattern of OR activation, odors are represented as spatiotemporally evolving activation patterns of different glomeruli (Mombaerts, 1999; Spors & Grinvald, 2002). This spatiotemporal activity constitutes the so called odor ‘maps’.

Under natural settings, animals are subjected to multiple odor plumes of varying concentrations, thus forming overlapping odor maps simultaneously. Also, similar odors form overlapping odor maps (Abraham et al., 2004; Rubin & Katz, 2001). The olfactory system employs various strategies for resolving overlapping glomerular patterns. However, the ability to resolve a single odor component comprised within multiple odors is highly dependent on the extent of overlap between the glomerular patterns (Rokni et al., 2014). Glomerular pattern separation is facilitated by circuitry downstream of the glomerular layer, which has been described below.

Within a glomerulus, OSN axons primarily form synapses with the principal output neurons of the OB (Shepherd & Greer, 1998), which are Mitral and Tufted cells (M/T). OSNs also form synapses with a group of interneurons collectively termed as juxtaglomerular (JG) interneurons (Figure 1). There are three types of identified JG:

External tufted (ET), Periglomerular (PG), Short axon (SA) cells (Pinching & Powell, 1971). These cells can be distinguished based upon their morphological as well as physiological characteristics. An ET cell is extensively arborized throughout a single glomerulus. Also, it does not have secondary dendrites extending into the External Plexiform Layer of the OB, unlike the tufted or mitral cells (Macrides & Schneider, 1982). A distinctive physiological feature of ET cells is their ability to generate rhythmic bursts of action potentials intrinsically without any rhythmic synaptic inputs (Hayar, Karnup, Shipley, et al., 2004). On the other hand, PG cells have a much smaller arborization as compared to ET cells around each glomerulus. Also, they are heterogeneous in the synaptic inputs they receive and the neurotransmitters released by them (Kosaka et al., 1998). SA cells form elaborate arborizations across multiple glomeruli, some located hundreds of micrometers away. OSN-evoked bursts of action potentials in ET provide excitatory input to PG and SA cells (Hayar, Karnup, Ennis, et al., 2004). Thus, ET cells act as a significant excitatory component in the glomerular network. Deeper in OB, beyond the glomerular layer, lies the external plexiform layer (EPL). M/T cells send several dendrites into the EPL, where they primarily form dendrodendritic reciprocal synapses with GABAergic granule cells (GCs). Structurally, a single mitral cell has a large cell body (~20µm), mainly extending its secondary dendrites to the deeper half of the EPL. On the other hand, tufted cells have medium to small cell bodies (~10-15 µm) distributed over the EPL and periglomerular region (Shepherd & Greer, 1998). They extend comparatively shorter secondary dendrites to the superficial half of the EPL (Nagayama et al., 2014). GCs are axonless neurons whose cell bodies are located in the granule cell layer and send their dendrites to the EPL (Shepherd & Greer, 1998). Upon activation, mitral cells release glutamate which bind onto the ionotropic glutamate receptors present on GCs' dendrites. This event leads to the release of gamma-aminobutyric acid (GABA) onto dendrites of the same (reciprocal inhibition) as well as neighboring mitral cells (lateral inhibition), in turn inhibiting surrounding mitral cell activity (Isaacson & Strowbridge, 1998). Reciprocal inhibition has been shown to play a role in regulation of the firing rate of M/T cells (Margrie et al., 2001). On the other hand, lateral inhibition has been shown to mediate contrast enhancement at the level of M/T cells by suppressing weakly activated M/T cells (Yokoi et al., 1995). Thus, they play a crucial role in the ability of odor discrimination in mice (Abraham et al., 2010). Hence, the OB consists of an elaborate organizational circuitry which crucially affects olfactory information processing. M/T

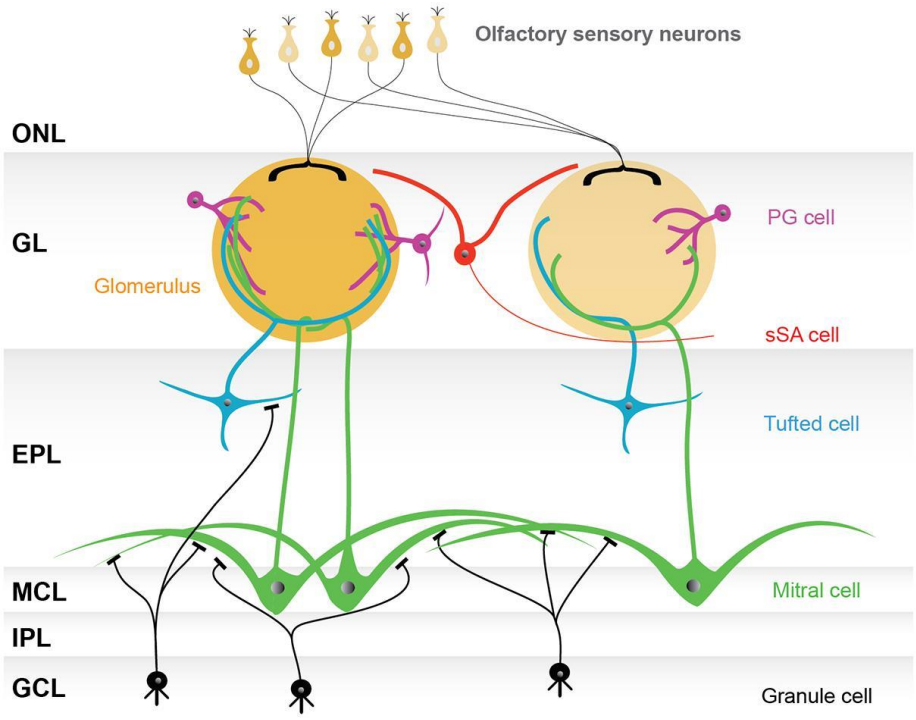

Figure 1: Neural organization of rodent olfactory bulb

cell activation patterns are tightly correlated with opposing phases of the sniff cycle. Thus, M/T cells fire in a phasic manner instead of firing simultaneously, during active odor sampling. This phase locking is facilitated by the selective delay of mitral cell activity due to locally induced inhibition by the interneurons both at the glomerular and granule cell layer. Therefore, tufted cells are activated first by odors, whereas mitral cell responses show a graded phase advance (Fukunaga et al., 2012).

M/T cells send their axons to different parts of the olfactory cortex. The primary olfactory cortex consists of regions classified based upon monosynaptic inputs from the OB. The anterior olfactory Nucleus, Piriform cortex (PCx), Olfactory tubercle, anterior cortical nucleus of the amygdala and periamygdaloid cortex, entorhinal cortex and accessory olfactory cortical areas (Price, 2009). MTCs send diffused overlapping projections to Layer II of the piriform cortex where they form synapses with pyramidal neurons (Miyamichi et al., 2011). As different sets of MTCs simultaneously project to PCx in a diffused fashion, pyramidal neurons in the piriform cortex receive signals from various simultaneously activated glomeruli (Davison & Ehlers, 2011). Hence, the spatiotemporal map formed in the bulb is sparsened in PCx (Miura et al., 2012; Stern et al., 2018; Stettler & Axel, 2009).

2.3 Encoding temporal aspects within odor plumes

Odorant molecules transported through plumes evolve non-linearly over space and time. Hence, an odor stimulus reaching the nostril of rodent is subject to unpredictable spatiotemporal fluctuations which are determined by a variety of features like the local temperature, pressure, humidity, etc. Thus, the olfactory system has to overcome the herculean task of resolving such convoluted data to filter relevant olfactory cues. Under environmental settings, the olfactory system is challenged to discriminate between odors embedded within highly fluctuating odor plumes.

For instance, if a predator is approaching a rodent, the odors emitted by the predator will not themselves change. However, there will be temporal changes in the identity of odor plumes reaching the prey's nose. In such a scenario, analyzing the olfactory scene will involve spatial as well as temporal components of the odor plumes. A prominent component which would vary with a progressing odor plume is the concentration of the odor within it. A recent study provided a direct evidence that the olfactory system has a mechanism for enhancing temporal contrast in varying concentrations. The study reported that a particular group of M/T cells could represent minute changes in odor concentrations between consecutive inhalations (Parabucki et al., 2019). It also illustrates the link between processes happening at the periphery (sniffing), and the downstream circuits which encode those processes (M/T cells).

Other than concentration fluctuations within odor plumes, some studies indicate that the rodent olfactory system can code for the duration of stimulus presentation window itself (Frasnelli et al., 2006; Li et al., 2014). Further, it was reported that the rodent olfactory system is robust enough to detect stimuli varying with stimulus duration differences as low as ~10ms (Li et al., 2014).

Odors originating from sources placed nearby, co-fluctuate in their concentration, whereas those which arise from distant sources are mostly uncorrelated. Based on the above hypothesis, it has been reported that animals can indeed detect these phase differences between the concentrations of the odorants and might use it for odor source localization (Erskine et al., 2019).

A yet another temporal feature in odor plumes that might carry important information is the timing of the glomerular activation with respect to a reference point. In this context, the stimuli are identical in their chemical nature but encountered after different

delays from a standard time reference. It has been shown using optogenetic stimulation (so called 'virtual' odor presentation) at the glomerular layer, that mice can reliably differentiate between identical stimuli presented at different time points during a sniff cycle. It was demonstrated (using optogenetics) that even a single glomerulus activity at different timings during a sniff cycle is enough to transmit necessary information for stimulus discrimination. Mice could differentiate timing differences as low as 25 ms apart (Smear et al., 2013). Further, it was also shown that optogenetic stimulation of M/T cells at different timings can also transmit temporal information contained within glomerular activation timings. It was also exhibited that such temporal information can be perceived by rodent olfactory system regardless of tiling with respect to sniff-time (Rebello et al., 2014).

In a recent study on humans, the same two odor components were delivered in a specific order or the reverse of that. It reported that, in humans, high fidelity coding of timing (as in mice) could not be demonstrated at a behavioral level (Perl et al., 2020).

Thus, although there are studies involving optogenetic stimulation to evoke temporally precise activations with different timings in rodents, no studies have tried to use the delivery of stimuli under more natural contexts. We intuited that, if the olfactory system can distinguish between timing of virtual odors presentation (Rebello et al., 2014; Smear et al., 2013), then, can the system also distinguish between timing of natural odor presentation. By that reasoning, if we deliver the same odor plume, at different timings, rodents should be able to sense that and perform a discrimination task based upon that timing cue. Therefore, we designed a Go/No-go based timing discrimination task.

Before we challenged the mice with a temporally complex task, like discriminating timing, it was essential for them to get used to the procedural aspects of the task. Therefore, we began by delivering two complex enantiomers at two different timings. Further, we sequentially reduced odor dissimilarity leaving only the timing as the discriminatory parameter. In the first phase of our experiments, all the 12 animals learn tasks that involved the delivery of distinct odors or odor mixtures. However, only 7 out of 12 animals learned the task involving only timing discrimination.

3 Materials and Methods

3.1 Test Subjects and Laboratory Conditions

Sr. No.	Experiment Phase	Animal Strain	No. of animals	Age	Status
1.	Phase 1	C57BL6/J	12	6-8 weeks	Finished
2.	Phase 2	C57BL6/J	10	6-8 weeks	Ongoing

Table 1: Test Subject Details

A total of 22 male C57BL6/J mice have been used for this study (Table 1). Animals were maintained on a 12-hour Light/Dark cycle. They were housed in Individually Ventilated Cages (IVC) which are continuously monitored for their temperature (25-27^{o}C) and humidity (45-55 %) levels. All the behavioral experiments are performed during the light cycle. The mice had free access to food but were kept on a 12-hour water deprivation cycle during the training period. The weights were regularly monitored during the training period and care was taken to ensure that weight doesn't fall below 80% *ad libitum*. All the animal care and procedures were done following the ethics and guidelines of the Institutional Animal Ethics Committee (IAEC) (IISER/IAEC/2019-02-05) and Committee for the Purpose of Control and Supervision of Experiments on Animals (CPCSEA), Government of India.

3.2 Odors used

All the odors used are provided by Sigma-Aldrich®. All the odors used during the course of experiments are listed below:

Phase 1:

1) (+)-limonene
2) (-)-limonene
3) (+)-carvone
4) (-)-carvone
5) (+)-octanol
6) (-)-octanol
7) Amyl acetate

Phase 2:

1) 2-pentanone

For studies involving different odors coupled with different timings, we have chosen the odor pairs based on the separation between the glomerular patterns elicited by the odors and the vapor pressure of odor (Figure 7). The idea was to optimize the complexity of the task by selecting odors which evoke partially overlapping glomerular pattern. Odors having equal vapor pressures were selected to minimize any discrepancy between their velocity during odor delivery.

3.3 Paradigm

We employed a modified **Go/No-Go** operant conditioning paradigm. In a traditional **Go/No-Go** (Figure 2) conditioning paradigm, animals are supposed to lick for a **Rewarded (S+)** trial to receive a reward and not respond for a **Non-rewarded (S-)**.

We were using an 8-channel custom built olfactometer similar to one used in (Abraham et al., 2004). The olfactometer operates based on a custom-written program using IgorPro, Wavemetrics. The program was custom modified to suit our experimental

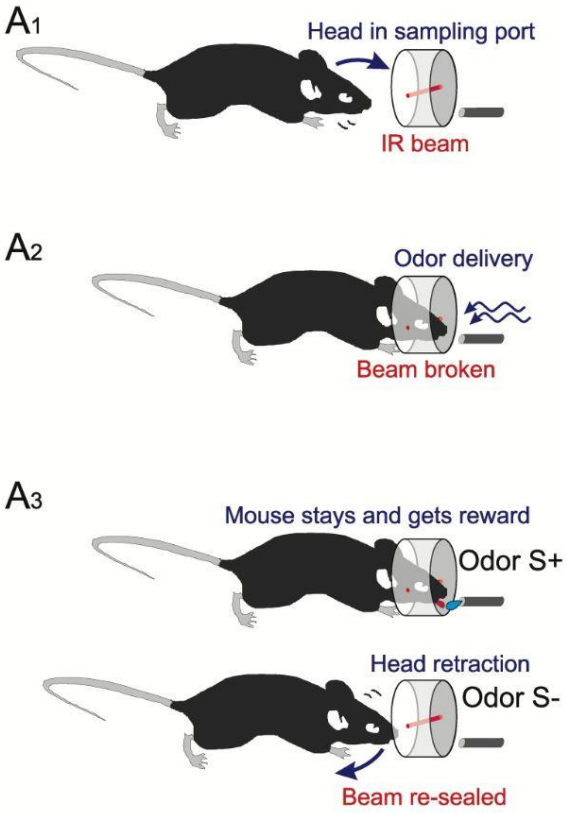

Figure 2: Go/ No-go paradigm (Figure adopted from Abraham et al.,2004)

(A1). IR beam breaks as soon as animal pokes its head

(A2). Beam break initiates task and background odor delivery

(A3). Animal receives the reward if it performs correctly for a rewarded trial; for non-rewarded trial, animal retracts its head

protocol. Following are the components of olfactometers used (Slotnick & Restrepo, 2005):

1. Flowmeters: Two glass flowmeters, one for monitoring clean air flow and another for monitoring odorized air flow. Both have stainless steel floats.
2. Glass and Teflon needle valves for controlling air flow through the clean and odorant control flowmeters.
3. Odor-saturator bottles: Here we have used 50 ml glass bottles from Borosil Glass Works Ltd.
4. Custom made glass manifolds: Two cylindrical manifolds with each having eight legs. One manifold opens on both ends for carrying odorized air, another manifold for carrying fresh air. Each output of the leg is connected to a single saturator bottle via separate solenoid valves. Each saturator bottle has two tubes, one for pumping in clean air, and another for carrying out odorized air.
5. Solenoid valves: Odorant solution in each saturator bottle isolated by a 2-way, default state closed solenoid pinch valve.
6. A mixing glass chamber: For ensuring the proper mixture of odorized and clean air before delivery.
7. Final Valve (FV): A three-way pinch valve which controls the flow of odorized air between the mixing glass chamber to the sampling port. Under default conditions, it directs the flow of odorized air to an external exhaust. Only during stimulus presentation, it shunts the flow to external exhaust and delivers the odorized air into the sampling port for a designated time and then returns to default state.
8. Reward: Water reward is delivered from a reservoir via a Tygon tube connected to the lick-cum-reward port A high fidelity solenoid valve monitors water delivery. 3 µl of water is delivered for a correct response towards rewarded trials.
9. Connecting tubes: All connecting tubes for glass-to-saturator bottle and glass-to-glass connections are 6-mm o.d., 3-mm i.d. C-flex tubing (Cole- Parmer).
10. Operant Chamber: Operant chamber made of Plexiglas with a vertically sliding door in the front. The left wall of the operant chamber contains a ventilation fan (directed inside) for chamber powered independently by a 12V, 1A power

adapter. The fan prevents the accumulation of odorized air in the operant chamber.

11. Odor sampling port: For Phase-1 experiments, odor port has four equilaterally placed holes for odor delivery and lick port to receive water reward (Figure 3).
12. Exhaust for sampling chamber: Exhaust for the sampling chamber located above the sampling chamber and clears the sampling chamber of any lingering odors after odor presentation.
13. Air supply: Main air supply is set at ~ 2 litres/min which is diluted further 20 times. The final odorized air flow reaching the animals is 400 ml/min.

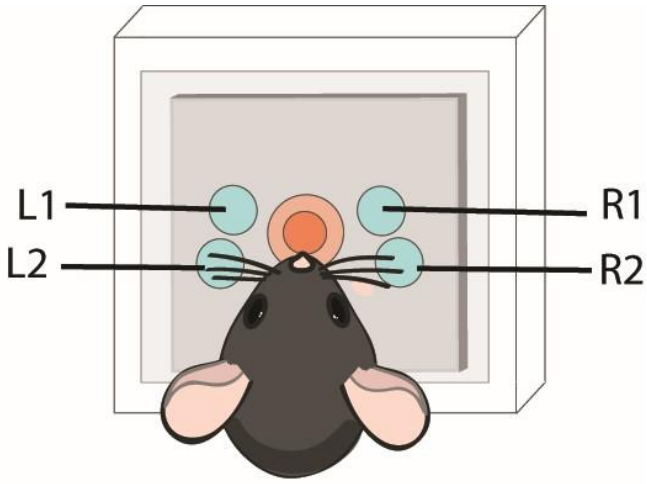

Figure 3 : Odor plume delivery system

The trial initiation is registered via an IR beam and a photodiode which guard the sampling chamber opening. The beam is broken when mice insert its head in the sampling chamber, thus initiating the trial. The stimulus odor delivery is controlled by valves that open for a defined amount of time (in Phase 1, for 500 ms). The order of rewarded and non-rewarded trials is pseudo-randomized. A valve does not isolate the saturator bottle corresponding to the furthermost valve from right. This valve is used for background odor for ensuring flow of background as soon as FV opens.

3.4 Experimental protocol

For achieving the goal of keeping odors the same but delivering them with different delays, we had to make some major modifications in the trial protocol as given in Abraham et al., 2004. The overall nature of the task is same, wherein the animal gets a reward for a rewarded trial upon performing appropriately, however, to ensure that animals use the temporal delay as a discriminating factor, we decoupled the sampling and the reaction window. While decoupling, we did not introduce any punishment that

would prevent animals from licking during the odor presentation. As the animals would have to lick for an extended period if they started licking during sampling period, we expected the animals to learn to not lick before the onset of reaction window. To mark the onset of reaction window, we played a tone for 200 ms. With this modification, we expect the animals to discriminate between the two stimuli on the basis of temporal delays and not using the perceptual differences in the odor as a discriminating factor. We tried to mimic a natural scenario wherein rodents have to pick relevant olfactory cues against a background odor.

The complete stimulus window was set for 2.5 s long. On trial initiation, the background odor was presented which continued for the entire stimulus duration. The animals were expected to detect the timing of target odor delivery in presence of the background odor. Based upon the nature of the trial, **S+** or **S-**, target odor was delivered in form after 500 ms or 1000 ms respectively, after the trial onset. The target odorants were mixed with mineral oil to a final concentration of 1% or 2% (mentioned accordingly in the results section). The background odor concentration was kept 1% throughout the course of all experiments in Phase-1. On initiation of a trial, FV opens, thus introducing a continuous flow of background odor. Depending upon the nature of the trial (**S+** or **S-)**, target odor valves open for 500 ms after the corresponding delays associated.

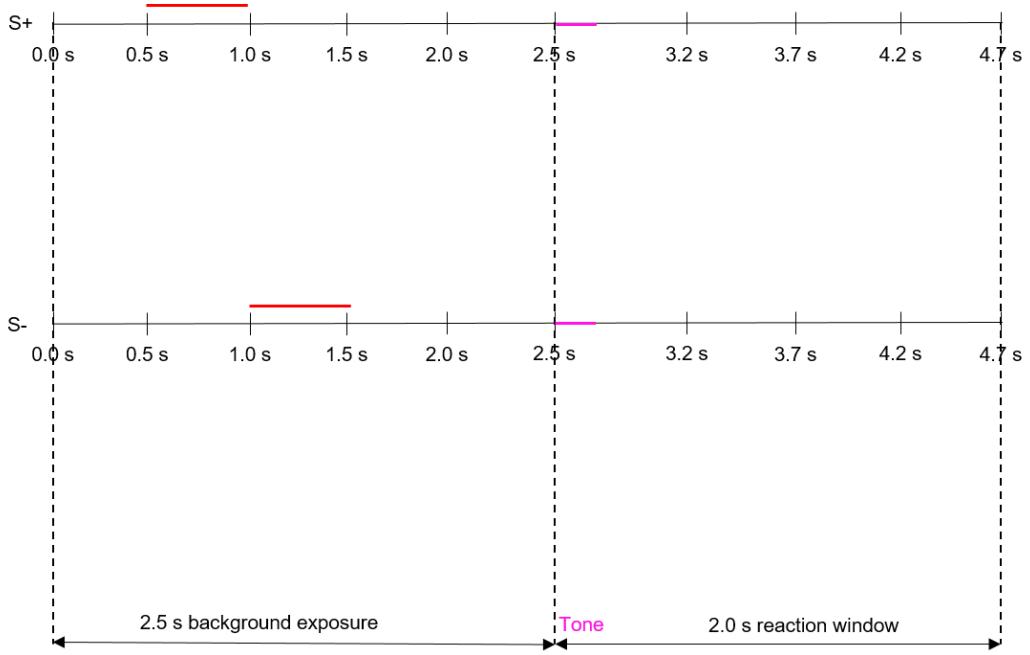

Figure 4: Schematic for Phase 1 protocol; Non-rewarded stimulus is delivered at a later timing than rewarded stimulus. The duration of the tone is 200 ms. Total duration of the trial is 4700 ms.

The target odor is delivered as a pulse amidst the background odor. The schematic of the protocol is given in Figure 4.

PID: The two odor channels are placed adjacent to each other for minimizing the differences in their travel times. The additional time beyond the offset of the stimulus in both cases is kept so that the animals don't associate the time from offset of the target odor to the tone as a potential cue to perform the trial. The reaction window is split in 4-time bins, each of 500 ms. For a S+ trial to be registered as correct, the animal should lick for at least 3 time bins. While for a S- trial to be registered correctly, the animal should either not lick or lick in 2 time bins at most. To make sure that opening valves at two different timings, odors are indeed delivered after different delays, a Photo-ionisation diode (PID) was used to get the signals for odor delivery,

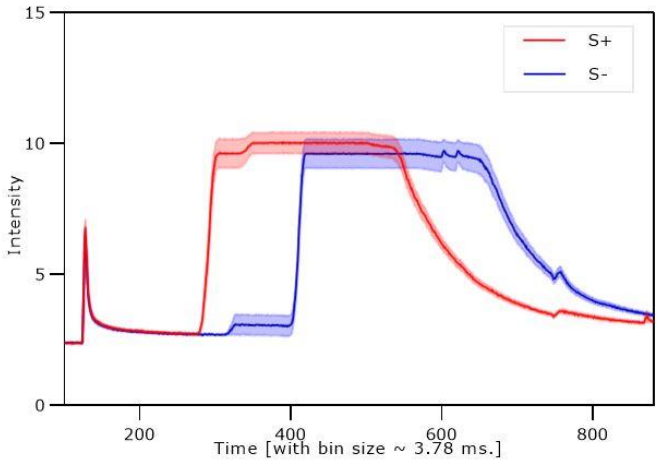

Figure 5: PID signal for Phase 1 protocol; Trace for rewarded stimulus rises at an earlier time point than that for non- rewarded stimulus.

as they are delivered inside the sampling chamber. The result for the same are given below (Figure 5). The choice of odors we used were selected based on their discriminability against background by comparing the odor evoked glomerular patterns for both.

3.5 Analysis

Every experiment is grouped into 'tasks', with each 'task' containing 300 trials. Each file has multiple arrays consisting data registered during training.

3.5.1 Learning Curve

Every task comprises of 150 rewarded and 150 non-rewarded trials. These trials are pseudorandomised in blocks of 20 trials. Each block consists of 10 rewarded and 10 non-rewarded trials, with not more than 2 repetitions of the same kind. Accuracy for

each block is calculated by averaging separate accuracies, over only rewarded trials and then, over only non-rewarded trials. That gives us a resultant accuracy for each block. Later, the block accuracies over 5 blocks are averaged to get an accuracy value over 100 trials.

3.5.2 Sampling Response

Animals have to enter the odor presentation chamber (also known as sampling chamber) to receive the stimuli and they actively sample the incident odor plumes. Hence, studying how sampling pattern varies throughout the learning might provide insights into the sampling strategies employed by the animals as they learn to perform with higher accuracy. We are specifically interested in looking at the difference between sampling response for rewarded vs. that for non-rewarded trial. Conventionally, sampling responses are observed by averaging for a task. The complete duration of trial of 4700 ms is divided into bins of 20 ms each. Thus, there are 235 bins with each bin having a decimal value between 0 to 1. For plotting the sampling response for a particular task, we compare bin wise averages over 150 **S+** and 150 **S-** trials. A representative sampling response curve is given in Figure 6A.

3.5.3 Licking Response

In a Go/No-Go odor/timing discrimination task, another response that gets registered with learning phenotype is licking response. As licking is the proxy for the animal to decide if the trial is rewarded or not, the nature of licking response could serve as a suitable proxy to find the time point when the animal has made its decision. Thus, similar to sampling response, we can find PoDs based on licking response. The analytical procedure is same as that for finding sampling response, as mentioned above. A representative licking curve is given below (Figure 6B).

3.5.4 Computing PoDs

Based on if we are calculating PoD from licking response or sampling response, the PoD can be calculated using a bin-wise one tailed paired t-test between **S+** and **S-** trials. A p-value (Figure 6B) curve is obtained from the p-values obtained by the above comparisons. The last time point where the p-value falls below a statistically significant value (marked with a black arrow in Figure 6B is considered the PoD. Given in Figure 6A is a licking response curve and Figure 6B is the corresponding p-value curve. An illustrative sampling response curve is given in Figure 6C. The values can be calculated for every task to get an idea of how the learning is progressing. As animals

learn the task successfully and reach more than 80% accuracy consistently, the PoD value obtained for these high accuracy blocks is taken as the PoD value corresponding the discrimination task.

3.5.5 Discrimination times (DTs) and Point-of-Discrimination (PoD)

Discrimination time is the time that the subject requires to discriminate between presented stimuli. Conventionally, in a Go/No-Go task discrimination times can be calculated based on the licking behavior. But, in case of odor stimulus being delivered at different timings we can't predict which part of the information is the animal using to differentiate. Therefore, as we consider the time point where the licking response for rewarded trial separates significantly from that for non- rewarded trials, we are calling it as Point-of-Discrimination (PoD).

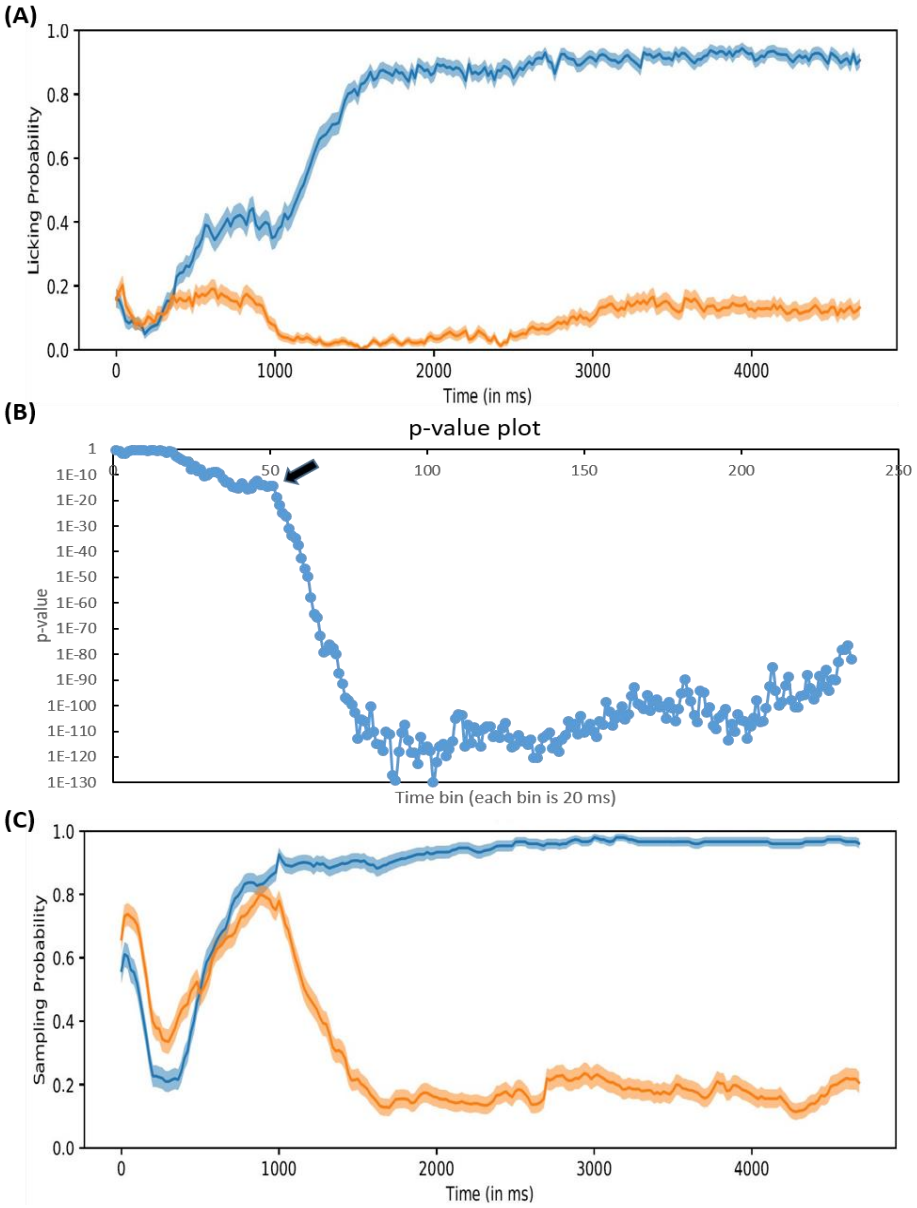

Figure 6: Illustrative plots used in evaluating behavioral response of animal

(A) Illustrative licking response curve of a learned animal

(B) P-value curve corresponding (A)

(C) Illustrative sampling response curve of a learned animal (only for representative purpose)

4 Results

In recent years, interest is brewing in the olfaction scientific community to understand whether animals can differentiate between odors arriving in close time intervals. A recent study with human subjects attempted to address this issue. In their study model, human participants were asked to differentiate between a pair of odor mixtures composed of two odors delivered in either one temporal order or its reverse (A followed by B vs. B followed by A), in rapid intervals (Perl et al., 2020). The subjects could hardly discriminate between the odor mixtures. This result raises speculation over past studies in rodents which suggest that time related information could be encoded in form of odor perception. One such study was in mice where glomeruli were artificially stimulated at different time intervals using an optogenetic approach. It was shown that rodents could discriminate delays of even 25 ms in glomerular activations with high accuracies, (Smear et al., 2013). However, such optogenetic stimulation may not necessarily mimic the activation of glomeruli by natural stimuli. Thus, conflicting results across different model systems make temporal coding by olfactory system a topic of immense interest. Therefore, in an attempt to reach consensus about coding temporal delays by olfactory system, we devised a strategy wherein animals were trained to differentiate between the same odor presented at different time intervals. To resemble natural conditions and to increase the task complexity, odorants were presented in presence of an odor background. For a traditional Go/ No-Go odor discrimination task, it has been observed that, the average response times lie in the scale of a few hundred milliseconds (Abraham et al., 2004; Bhattacharjee et al., 2019; Resulaj & Rinberg, 2015). Therefore, while designing the task paradigm, we chose the duration of odor stimulus sufficiently long to spam the maximum time required by animals to make a decision. We decided to present the two odors for a duration of 500 ms separated by a delay of 500 ms. To start off, we wanted to keep the temporal delay sufficiently long to prime the animals to perform with high efficiencies. The final objective was to decrease the time delay to determine the minimum temporal delay that can be perceived by the olfactory system.

4.1 Experimental Timeline

4.1.1 Protocol

Two distinct odors (enantiomers) were delivered at two different timings amidst a background odor. In this experiment, animals need not rely entirely on the temporal

delay as the subtle difference in odors provide additional discriminability. This task was designed to train the animals on the procedural aspects of the task paradigm. This task paradigm deviates from the conventional Go/No-Go paradigm, as the animals need to wait during stimulus presentation and should only respond during the reaction window. A tone was played to indicate the beginning of the reaction window. With each experiment, the similarity between the target odor was increased with the ultimate goal to train animals to differentiate between the same target delivered at variable temporal delays. Note that the target odor was at a higher concentration to normalise the relative vapor pressure differences between target and background. However, this normalisation was not undertaken for first experiment.

Experiment 1: (+)-limonene (1%) vs. (-)-limonene (1%) as target odors, Amyl acetate (1%) as background. Although the enantiomer pair of limonene share high structural similarity, the glomerular activity patterns evoked by limonene enantiomers differ statistically and are perceived quite distinctly (Bhattacharjee et al., 2019; Linster et al., 2001) (refer Figure 7). Thus, we started our experiments with this particular odor pair.

Experiment 2: (+)-carvone (2%) vs. (-)-carvone (2%) as target odors, Amyl acetate (1%) as background (Figure 7).

Experiment 3: (+)-carvone [80%] + (-)-carvone [20%] (2% dilution) vs. (-)-carvone [80%] + (+)-carvone [20%] (2% dilution) as target odors, Amyl acetate (1%) as background.

Timings: Rewarded stimulus was presented with a 500 ms delay, while non-rewarded stimulus with 1000 ms delay.

4.1.2 Protocol:

Same complex mixture of two odors (enantiomers) delivered at two different timings amidst a background odor

Odors: (+)-octanol [80%] + (-)-octanol [20%] (2% dilution) as target odor, Amyl acetate (1%) as background.

Timings: When the target odor was presented with a 500 ms delay, it was regarded as rewarded stimulus, while presented with a 1000 ms delay, it was considered as a non-rewarded stimulus.

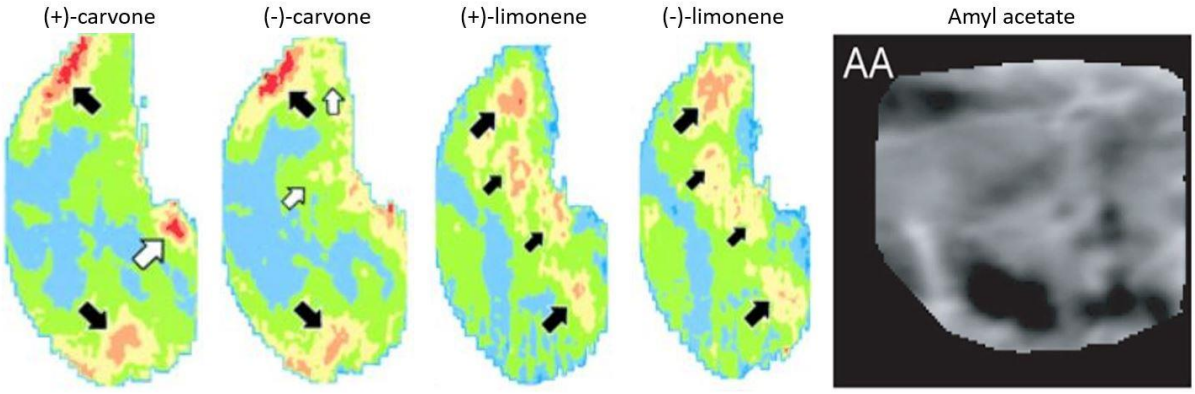

Figure 7: Glomerular patterns for odors used (figures adopted from: Linster et. al,2001 and Bhattacharjee et. al., 2019); Carvone enantiomers evoke more overlapping pattern as compared to limonene enantiomers

4.2 Mice readily learn to discriminate between monomolecular enantiomer pairs presented at different timings

We plotted the progression of learning in the form of a learning curve by averaging 100 trials. Learning curve (Figure 8A) for the first experiment involving (+)-limonene vs. (-)-limonene discrimination indicates that animals learned to perform the task with high accuracy (more than 80%) by end of 600 trials. However, accuracies crossed 90% only after 1000 trials. Such a learning behavior is indicative of the complexity of the task. For a traditional two odor discrimination task, animals reach high accuracies within 300 trials and chances of error reduce once they achieve high accuracies (Abraham et al., 2004; Bhattacharjee et al., 2019).

To determine the strategy employed by animals to perform this complex task, we probed the sampling and licking patterns of the animals while performing the task. The sampling and licking response can be a good indication of learning based upon the separation between the responses for rewarded vs. non-rewarded trials. The sampling response of one animal during the last task while performing with high accuracy is plotted in (Figure 8B). It can be seen that for rewarded trials, animals remain within the sample port to lick for water reward while for the non-rewarded trials, on arriving at a decision withdraw their head out of the port.

Similar to sampling response, the licking response (Figure 8C) for rewarded and non-rewarded trials also diverges from each other as the animals learn. Licking responses

for rewarded trials indicate increased licking once the animal understands reward value. On analysing the lick response we realised that animals barely waits for the beginning of the reaction time window and starts licking as soon as the first odor is presented. They follow the same action for non- rewarded trials, however in absence of odor during first time window, they recognise it to be non-rewarded trial and stop licking.

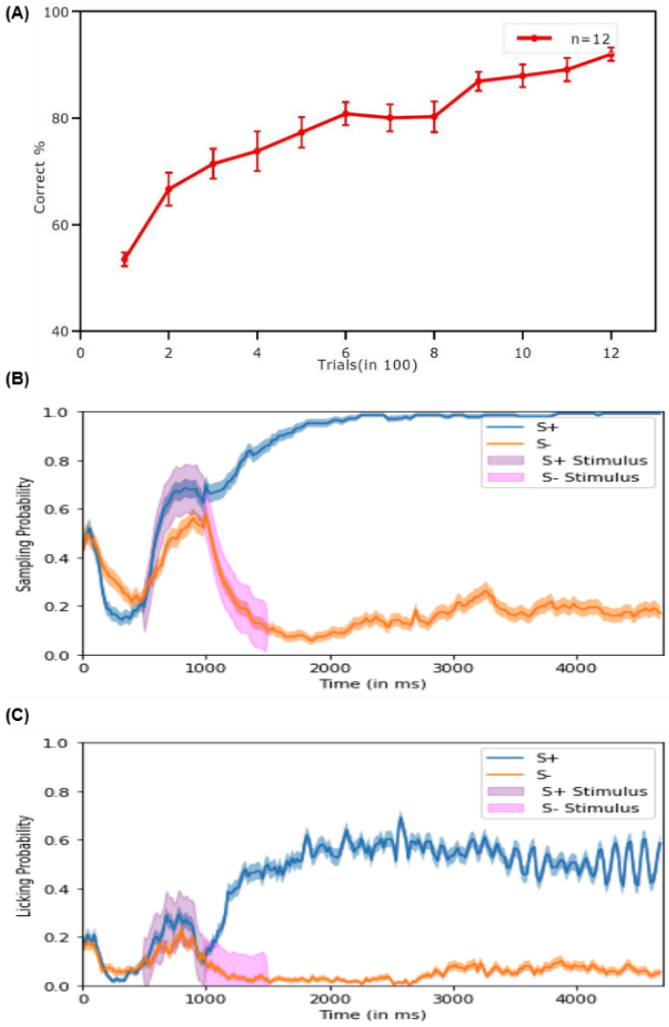

Figure 8:

(A). Learning curve for task involving discrimination between limonene enantiomers (1%) presented at different timings, with amyl acetate (1%) as background.

(B). Illustrative sampling response curve for an animal which has learned the task. The width of the spreads (marked in pink and magenta) indicating stimulus presentation window is arbitrarily set to 0.1 and serves the only purpose of indicating stimulus delivery window.

(C). Illustrative licking response curve for the same animal whose sampling response is illustrated in (B). The width of the spreads for indicating stimulus presentation window is same as above

Significant divergence in sampling/licking-responses for rewarded vs. non-rewarded stimuli indicates the decision making time point for stimuli. To study the evolution of

decision-making strategies during learning, we segregated the trials based on learning accuracies. Accordingly, trials were sorted in three categories: A) Blocks with accuracy less than 60%, B) Blocks with accuracy between 60% to 79%, and C) Blocks with accuracy equal to or more than 80%. A bin-wise average is calculated over all trials in each category. Representative accuracy wise sampling patterns for a single animal is depicted in (Figure 9(A-C)). We can observe that, for low accuracy trials, animals are unsure about the decision and keep entering into the sample port for non-rewarded trials. The indecisiveness is also illustrated in the licking response (Figure 9(D-F)) where the animal licks onto both rewarded as well as non-rewarded trials. In medium accuracy blocks, the indecisiveness reduces, as can be observed from the extent of separation in sampling and licking curves for rewarded vs. non-rewarded trials. With increasing accuracies, as the sampling and licking patterns begin to diverge considerably for rewarded vs. non-rewarded trials. For each animal we defined the point where the patterns diverge statistically as the Point-of-Discrimination (PoD). This point defines the decision-making time to perform the task.

The PoD calculated based on accuracy wise categories suggests that as animals learn the task and start performing with higher accuracy, their PoD shifts on a faster time scale. Accuracy wise PoDs calculated using licking response data are given in (Figure 9G). PoDs are calculated from the timing after the introduction of the rewarded stimulus.

For low accuracy trial blocks, there is no clear decision being made by the animals and thus the PoD is high and approaching 4000 ms. From the PoD values (Figure 9G), we can see that as animals learn the task, they discriminate between the stimuli much faster. A significant reduction in the mean PoD values across accuracy categories indicates the same ($n = 12$, RM one-way ANOVA, $p < 0.0001$, $F=22.17$; Tukey's multiple comparisons test ($p=0.0222$ for '<60' vs. '60 to 79', $p<0.0001$ for '<60' vs. '≥80 ', $p=0.0291$ for '60 to 79' vs.'≥80'). From the first experiment, the approach taken by the animals to perform the task is evident. Upon entering the sampling port, animals start licking immediately. If the rewarded odor arrives at 500 ms, they continue licking till they receive reward, while if the odor doesn't arrive within 500 ms, they reduce the licking. This can be illustrated by the dip in the licking probability before the onset of the non-rewarded trials (Figure 9(D-F)).

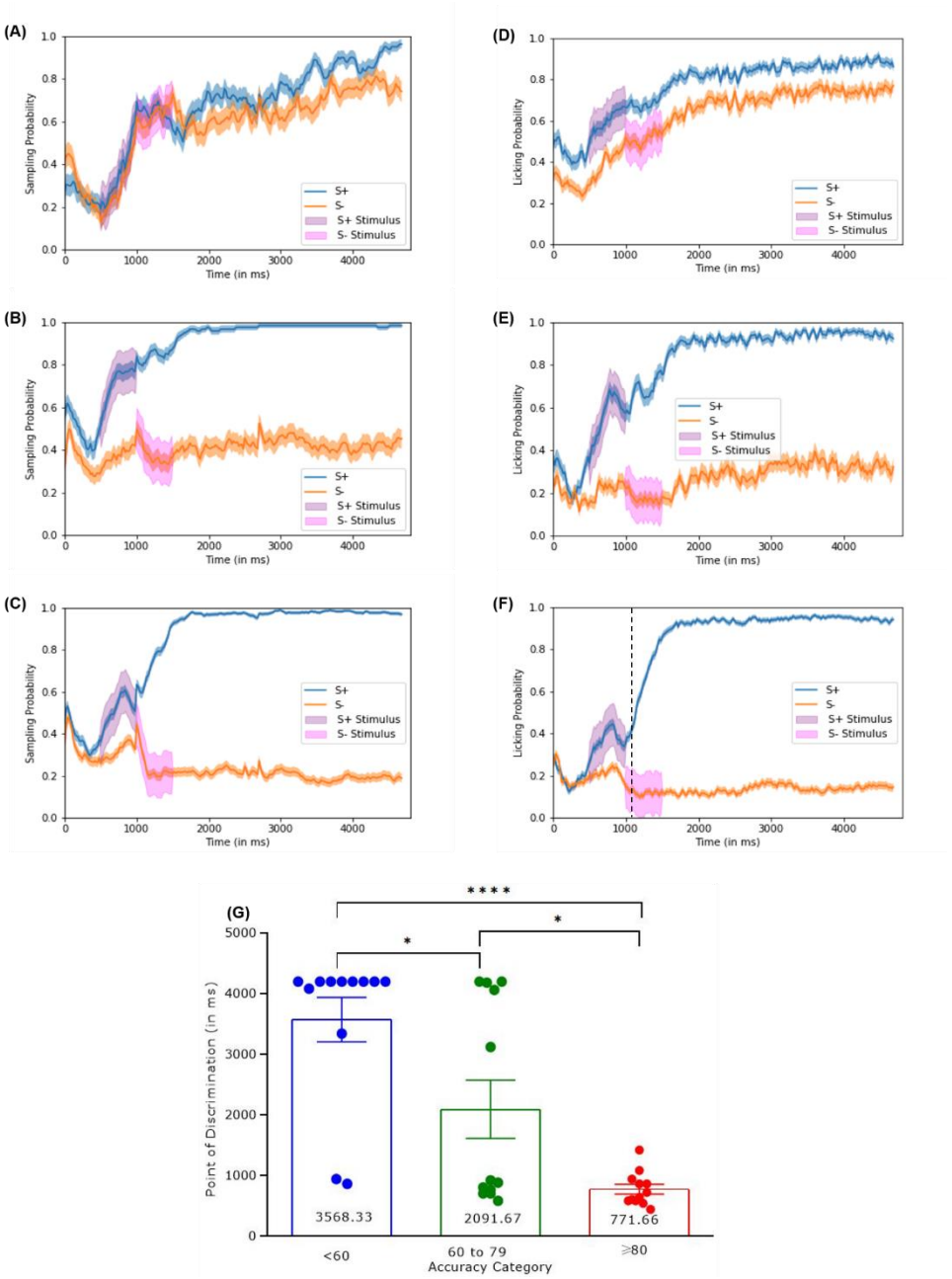

Figure 9: Visualizing evolution of sampling and licking behavior with learning

(A-C). Change in sampling behavior of an animal as it learns to perform the task with increasing accuracy; (A) Sampling curve for a naïve animal; (B) Sampling curve when the animal starts picking up some cue but still makes some mistakes, trace for rewarded trials separates from that for non-rewarded trials; (C) Sampling curve once the animal has learned to perform the task (≥80%) accuracy, trace for rewarded trials further separates and the span of SEM reduces, thus indicating lesser proneness towards committing mistakes; The width of the spread indicating stimulus presentation windows is arbitrarily set to 0.1

(D-F). Change in licking behavior of an animal as it learns to perform the task with increasing accuracy; (D) Licking curve for rewarded vs. non-rewarded trials when the animal is completely naïve, however we can see a small amount of separation from these traces, and that wasn't apparent from the corresponding sampling pattern in (A); (E) Separation in licking pattern for rewarded vs. non-rewarded further diverges; (F) Licking pattern for rewarded vs. non-rewarded further separates out and the span of SEM reduces, thus implying lesser proneness towards committing mistakes, PoD for this animal represented by black dotted line; The width of the spread indicating stimulus presentation windows is arbitrarily set to 0.1

(G). The point at which the licking pattern for rewarded trials diverge from that for non-rewarded trials reduces significantly as the animals learn the task; In most naïve animals (Blue column), as they are unable to discriminate between the stimuli, their PoDs are taken to be the end of the trial duration; As they learn to perform the task, the variability in their PoD, apparent in second case (Green column) reduces, as seen in the third case (Red column) (n=12, RM-One way ANOVA, $p < 0.0001$, $F=22.17$; Tukey's multiple comparisons test ($p=0.0222$ for '<60' vs. '60 to 79', $p<0.0001$ for '<60' vs. '≥80 ', $p=0.0291$ for '60 to 79' vs. '≥80'); The PoD described here are without considering the time (500 ms) before the timing of rewarded stimulus delivery

Although, the target odor was different in this first experiment, we got a glimpse of animals being able to detect the temporal delays in odor delivery. If the animals entirely relied on the odor differences, they would decide at two different times depending upon if the stimulus is rewarded or non-rewarded. However, the animals seemed to wait for a longer period, as measured by PoD measurements. This motivated us to increase the task complexity by increasing the similarity between the target odor.

4.3 Mice's performance in odor timing discrimination is similar across different odor pairs

Once we observed that animals started discriminating between temporal differences between odor onsets, to increase the task complexity, we started training the animals to Carvone enantiomers as target odors. On training the animals on these odors, we observed (Figure 10A) that animals reached more than 90% accuracy within 1200 trials (4 tasks). Comparing the learning curve (Figure 10B) for this task with that of the previous experiment with limonene as target odor shows that animals did not face any difficulty in learning to discriminate between odors eliciting more overlapping glomerular patterns (Ordinary two-way ANOVA, Sidak's multiple comparisons test, $p>0.05$, $p=0.9592$, $F=0.3902$). Along with learning, the sampling and licking response (Figure 9) from the last task was similar to the previous experiment. Briefly, task-wise sampling response curves of all animals show separation between rewarded and non-rewarded sampling responses. From the sampling response curve, we can say that the sampling for non- rewarded trials drops by the end of rewarded stimulus itself.

Upon careful observation of accuracy wise sampling (Figure 11(A-C)) curves, we can see that animals developed better sampling strategies quicker for this experiment than the previous one. This is evident if we compare the sampling response curves for

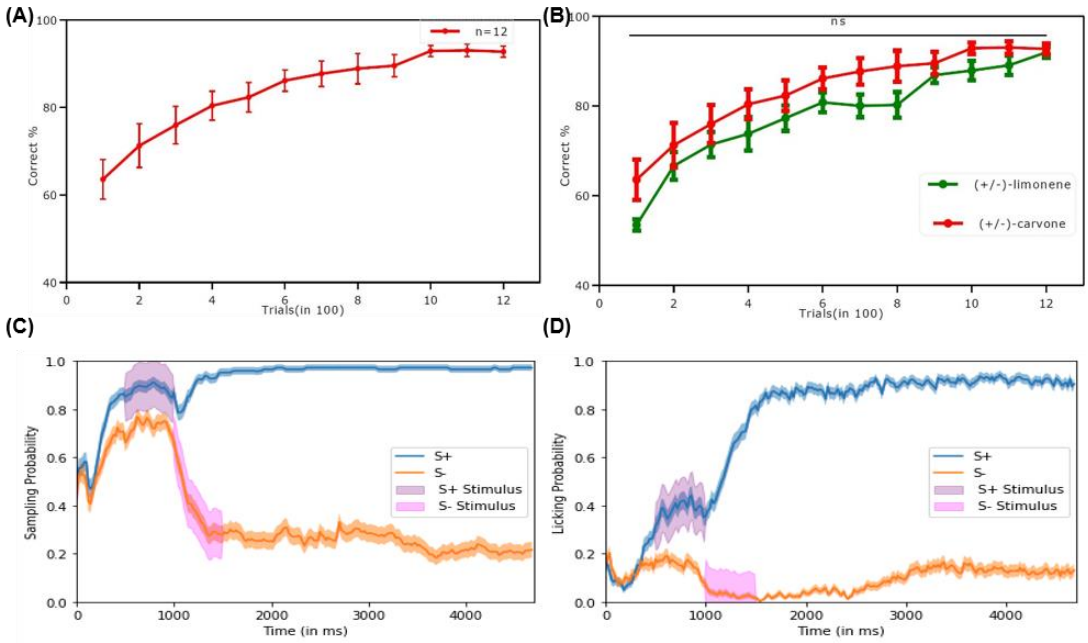

Figure 10:

(A). Learning curve for task involving discriminating between carvone enantiomers presented at two different timings, animals achieve more than 80% accuracy by 600 trials

(B). Comparison between learning pace of animals for discriminating between carvone enantiomers and limonene enantiomers, presented at two different timings, there is no significant difference between the learning pace (Ordinary two-way ANOVA, Sidak's multiple comparisons test, p>0.05, p=0.9592, F=0.3902), thus implying that animals readily learn to discriminate even between a more difficult enantiomer

(C). Illustrative sampling curve for a learned animal. Animal withdraws its head once it has made the decision, which is evident from the drop in sampling response curve

(D). Corresponding licking curve for the same animal as in (C), we can observe that even though the sampling remains high during the 500-1000 ms window, the licking is much lower during that window

second category (60% to 79%), we can notice that sampling responses for current experiment (Figure 11(A-C)) separate with a greater difference between response for rewarded vs. non-rewarded trace than that for the previous experiment (Figure 9(A-C)). A similar conclusion can be drawn considering licking responses for the corresponding experiments. Accuracy wise PoDs found from the licking response of animals are given in Figure 11G. As mentioned previously, the values of PoDs given in Figure 11G are without considering the first 500 ms of every trial. The PoD values (Figure 11G) indicate that, with learning, animals take a significantly faster decision (n = 12, Mixed-effects Analysis, p = 0.0001, F = 18.56; Tukey's multiple comparisons test (p=0.2037 for '<60' vs. '60 to 79', p=0.0001 for '<60' vs. '≥80 ', p=0.0091 for '60 to 79' vs. ' ≥80').

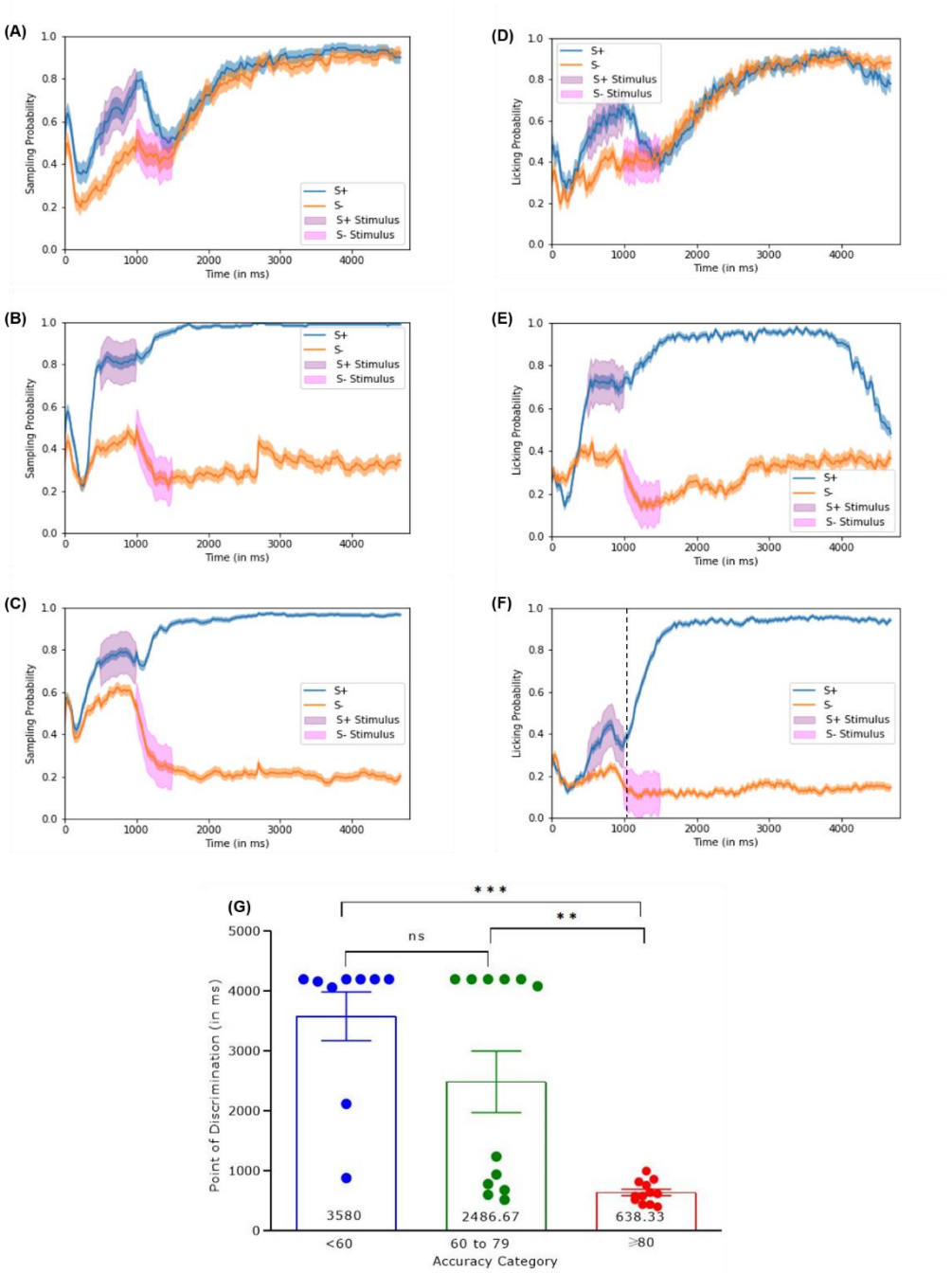

Figure 11: Visualizing evolution of sampling and licking responses as animals learn the task

(A-C). Sampling response curve of an animal as its learning progresses; (A) The sampling response for rewarded vs. non-rewarded trials is highly overlapping, indicating that the animal has yet not learned to discriminate between the two stimuli; (B) Sampling response curve begins to separate, although the span for non-rewarded trials is more than that for rewarded trials, indicating that the animal is still prone to commit mistakes for non-rewarded trials; (C) Sampling response curve further separates and the span for non-rewarded trials reduces indicating less proneness of the animal to commit mistakes; The width of span representing stimulus presentation window has been arbitrarily set to 0.1

(D-F). Corresponding licking response for the same animal as in (A-C); (D) Here, the licking curves show a coinciding trend as the one elicited by the corresponding sampling response in (A); (E) The licking response is diverging, albeit with the trace for non-rewarded trials exhibiting a similar larger span of SEM as seen in sampling of non-rewarded trials in (B); (F) The licking response for rewarded vs. non-rewarded trials separates clearly and the span of SEM for non-rewarded trial reduces, indicating a better learning of the task, PoD for this animal represented by black dotted line; The width of span representing stimulus presentation window has been arbitrarily set to 0.1

(G). The PoD of animals once they achieve high accuracy (≥80%) is significantly lower (n = 12, Mixed-effects Analysis, p = 0.0001, F = 18.56; Tukey's multiple comparisons test (p=0.2037 for '<60' vs. '60 to 79', p=0.0001 for '<60' vs. '≥80 ', p=0.0091 for '60 to 79' vs. '≥80'); The PoD values are computed without considering the initial period of 500 ms. during which there is not stimulus presented in either type of trial

4.4 Presenting similar odors at different timings increases the difficulty of discriminating between enantiomer mixtures

The learning performance from the previous two experiments indicate that animals had learned the procedural nature of the task. Therefore, we decided to increase the difficulty of the task further. We used complex mixtures of mixtures of (+)-carvone and (-)-carvone in a ratio of [80:20]. Hence, (+)-carvone [80%] : (-)-carvone [20%] was presented after 500 ms as a stimulus associated with rewarded trials, whereas (+)-carvone [20%] : (-)-carvone [80%] was presented after 1000 ms as a stimulus associated with non-rewarded trials. When the mice were trained on this odor pair, we observed that mice struggled to learn at the same learning pace as they had done for previous simpler stimuli. Within four tasks, animals could barely reach 80% accuracy levels. Even after reaching 80% accuracy, the performance kept fluctuating. This is evident by comparing the learning progression with the previous training set (Figure 12B) (Two-way ANOVA, Sidak's multiple comparisons test, $p<0.0001$, $F = 187.1$). Therefore, we decided to conduct one more task in continuation with these four tasks. However, there was a break of a few days before the next task was conducted. As different animals learned at a different pace, this break us to start the last task for all animals uniformly. This break has been represented by the break in the axis in learning curve for the set (Figure 12A).

Since similar odors evoke highly overlapping glomerular pattern (Abraham et al., 2004), resolving them becomes a more complicated task as compared to discriminating between just the enantiomer pair. In this case, we are using a mixture of carvone enantiomers, thus making the task more complex. However, even after this increased complexity, the rewarded and non-rewarded sampling (Figure 12C) and licking (Figure 12D) responses show divergence once the animals learn to perform the task.

From both, sampling and licking response curves, we can conclude that animals exhibited a slower pace of learning (Figure 12B) (Two-way ANOVA, Sidak's multiple

comparisons test, p<0.0001, F =187.1). However, once the animals learned to perform the task with high accuracies, their licking and sampling behavior significantly varied between rewarded and non-rewarded trials. Additionally, this animal started the licking response only after the presentation of the odor (Figure 12D). Further, it did not retract its head for the complete duration of a trial, as seen in (Figure 12C).

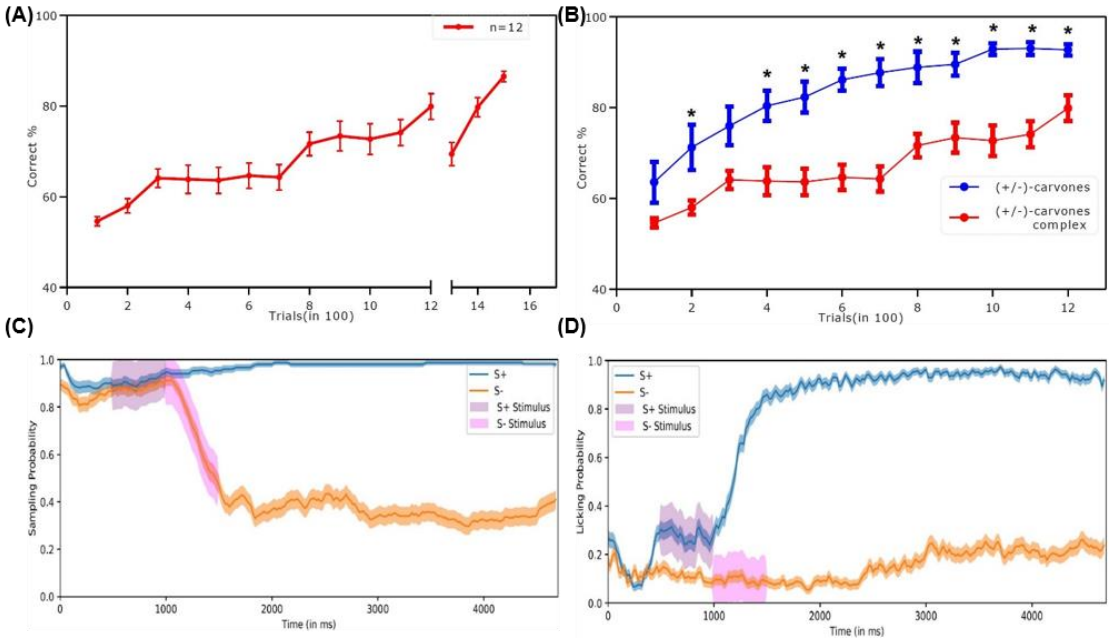

Figure 12:

(A). Learning to discriminate between similar odors proved a more difficult task, as can be seen in (B), for the animals to achieve more than 80% accuracy, an additional task had to be carried out, which is indicated with a break as there was a break of a few days before the additional task was performed

(B). Comparison of learning pace for this task with that of the previous task showed a significant difference in the learning pace of the animals at multiple points (Two-way ANOVA, Sidak's multiple comparisons test, p<0.0001, F =187.1)

(C). Illustrative sampling response of an animal when it learned to perform the task with high accuracy during the last task; we can see that the sampling response for non-rewarded trials shows a steep decrease, thus indicating that the animal has taken a decision; The stimulus delivery window is represented by a span of width 0.1 set arbitrarily

(D). Corresponding illustrative response of the same animal as in (C); As the sampling response for non-rewarded trials falls as depicted in (C), the licking response for rewarded trials increases eliciting the point of decision making; The stimulus delivery window is represented by a span of width 0.1 set arbitrarily

On plotting accuracy wise sampling responses of a learned animal, we can see a gradual decline in sampling for non-rewarded trials similar to previous experiments Figure 13(A-C).Accuracy wise licking responses of a learned animals are given in Figure 13(D-F). From the accuracy wise licking responses, we can clearly see that the licking behavior for a non-rewarded trial indeed falls once the animals learn to perform the task.

If we consider the accuracy wise sampling Figure 13(A-C) curves, the sampling response indicates that there is a difference in sampling strategy of the animal between rewarded and non-rewarded odor. We observe that the sampling probability is lower during 500-1000 ms window for non-rewarded trials as compared to that for rewarded trials. This discrepancy implies that animals were withdrawing their heads

prematurely, resulting into wrong sampling. Due to erratic sampling, animals were re-entering and licking indiscriminately for both stimuli. The complexity of the task can be probable reason for such erratic behavior.

The mean PoD values for category B and C in Figure 13G show a statistically significant difference (PoD means: B = 730.909, C = 572.727), which means that animals were significantly faster at discriminating between stimuli when they had learned the task well (n = 11, RM one-way ANOVA, p =0.0009, F=21.34; Tukey's multiple comparisons test (p=0.0031 for '<60' vs. '60 to 79', p=0.0019 for '<60' vs. '≥80 ', p=0.0375 for '60 to 79' vs. ' ≥80').

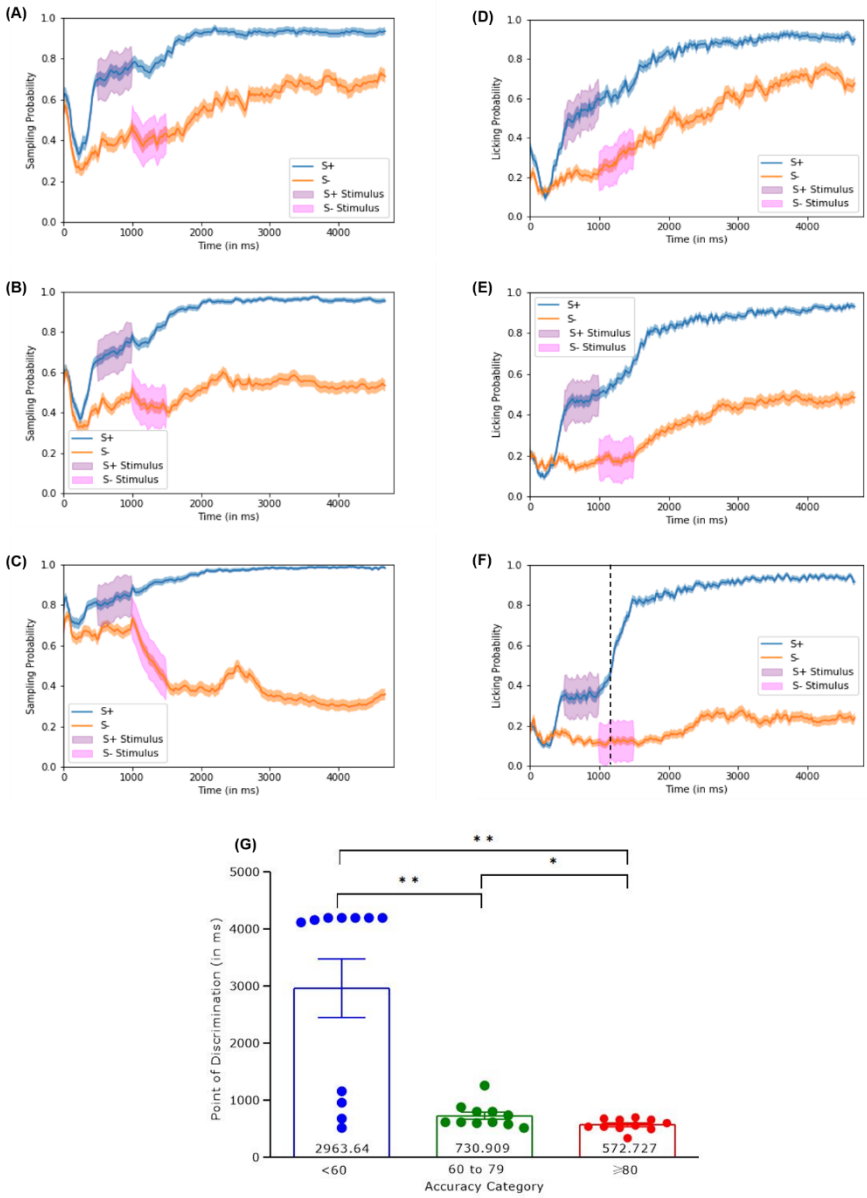

Figure 13: Visualizing sampling and licking response for task involving discriminating of between similar odors presented at two different timings

(A-C). (A) Sampling response for rewarded and non-rewarded trials is not very overlapping as observed for lower accuracy blocks in previous experiments, yet it takes substantial learning for further separation;(B) Sampling response for this case indicates that the animals were sampling less for non-rewarded trials and such improper sampling might be able to explain the slower learning pace of animals during this task; (C) Sampling response after the animal has learned however, indicates that once the animal learns to perform the task it exhibits similar phenotype of committing less mistake for non-rewarded trials as seen in previous experiments; The span of stimulus delivery window is arbitrarily set to 0.1

(D-F). (D) Licking response, similar to corresponding sampling response in (A), shows some separation even for low accuracy trials; (E) The licking response shows a similar trend to corresponding sampling response in (B); (F) As observed in previous experiments, here also we can observe that once the animal learns the task, the increase in licking response for rewarded trials is steep, PoD for this animal represented by black dotted line; The span of stimulus delivery window is arbitrarily set to 0.1

(G) From the PoDs we observe that the PoD reduces in the second case itself (Green column), indicating that animals are able to discriminate between the trials, yet they are prone to commit mistakes probably due to the complexity of the task; Although, once they learn the task achieving high accuracy (≥80%), their PoD significantly reduce further (n = 11, RM one-way ANOVA, p =0.0009, F=21.34; Tukey's multiple comparisons test (p=0.0031 for '<60' vs. '60 to 79', p=0.0019 for '<60' vs. '≥80 ', p=0.0375 for '60 to 79' vs. '≥80')

4.5 Discriminating between same odor delivered in close time interval is extremely difficult

Finally, when animals started performing previous experiment task with high accuracy, we progressed to the next phase of training by choosing same target odor with temporal delays. For this set, we chose a complex mixture of (+)-octanol [80%] : (-)-octanol [20%] as the target odor. Thus, the target odor was delivered at two different timings, 500 ms for rewarded and 1000 ms for non-rewarded. It is evident from the learning curve (Figure 14A) that animals could attain high enough accuracy

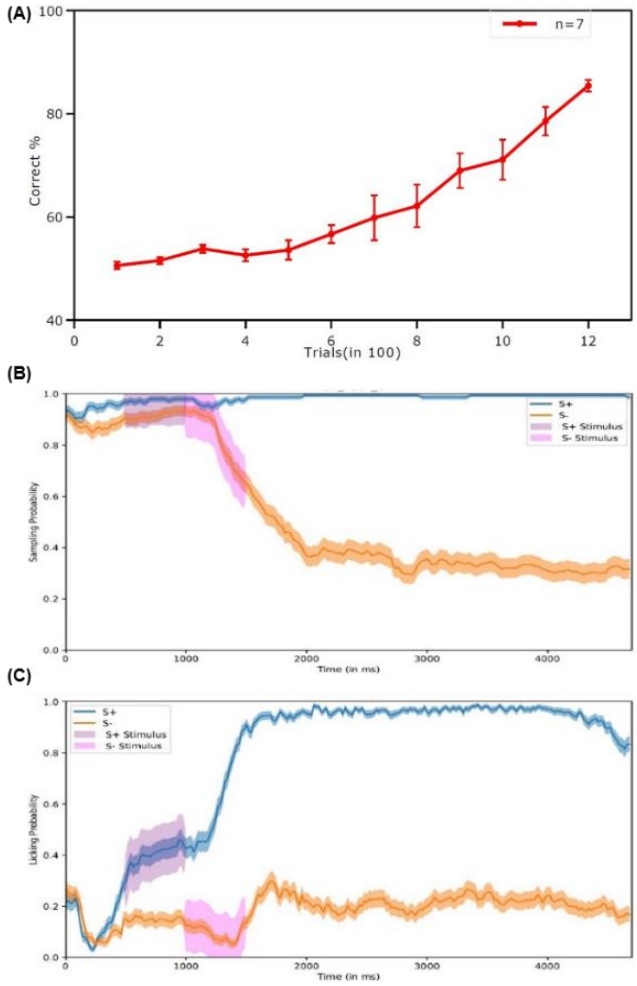

Figure 14:

(A). Learning curve of animals which were able to learn the task of discriminating between timings of same odor presentation indicates that they achieved high accuracy (≥80%) in 1100 trials, however only 7 out of 12 animals could learn the task

(B). Illustrative sampling response indicates a steep fall in the trace for non-rewarded trials indicates that the animal has learned the task properly; The spread for stimulus delivery window has a width of 0.1 set arbitrarily

(C). Illustrative licking response of the same animal as in (B) shows a steep rise in licking response for rewarded trials, similar to what has been observed in previous experiments; The spread for stimulus delivery window has a width of 0.1 set arbitrarily

towards the end of the 4th task. However, out of twelve animals, only seven could learn the task with high accuracy by the end of 4 tasks. The learning curve contains values only from those animals which learned the task successfully.

Once animals started learning during the latter half of the last task, the task wise sampling (Figure 14B) and licking (Figure 14C) were plotted and the responses show divergence between the responses for rewarded and non-rewarded trails for the last task.

The accuracy wise sampling (Figure 15(A-C)) and licking (Figure 15(D-F)) plots below are of an animal that learned the task later as compared to other animals. From the sampling and licking responses, we see a gradual separation between rewarded and non-rewarded trials. However, the sampling response looks much more discernible as compared to the licking response. A probable reason can be that due to the familiarity with the procedural aspects of the task, the animal can optimize its sampling strategy based on previous training experience. However, when it comes to licking consistently for rewarded trials, the animal might not be confident enough with the decision to elicit a consistent licking response, as it does in previous experiments. This could be a result of the complexity of the task wherein, the animals are not able to conclude the nature of the trial based on the timing of odor presentation. Yet they take a decision motivated by the reward contingency.

From the accuracy wise PoD values in Figure 15G($n = 7$, RM one-way ANOVA, $p=0.0288$, $F=9.091$; Tukey's multiple comparisons test ($p<0.2115$ for '<60' vs. '60 to 79', $p<0.0033$ for '<60' vs. '≥80 ', $p=0.2548$ for '60 to 79' vs. ' ≥80')), we can observe that even for such difficult task of discriminating odor timing, some animals are able to learn the task.

Thus, the results for above mentioned experiments suggest that animals can detect temporal delays when provided with similar odor. However, if they are subjected to identifying temporal delays within the presentation of the same odor, their learning varies from animal to animal, as we saw that only seven out of twelve animals were able to learn the task. A possible reason is discussed later in the thesis.

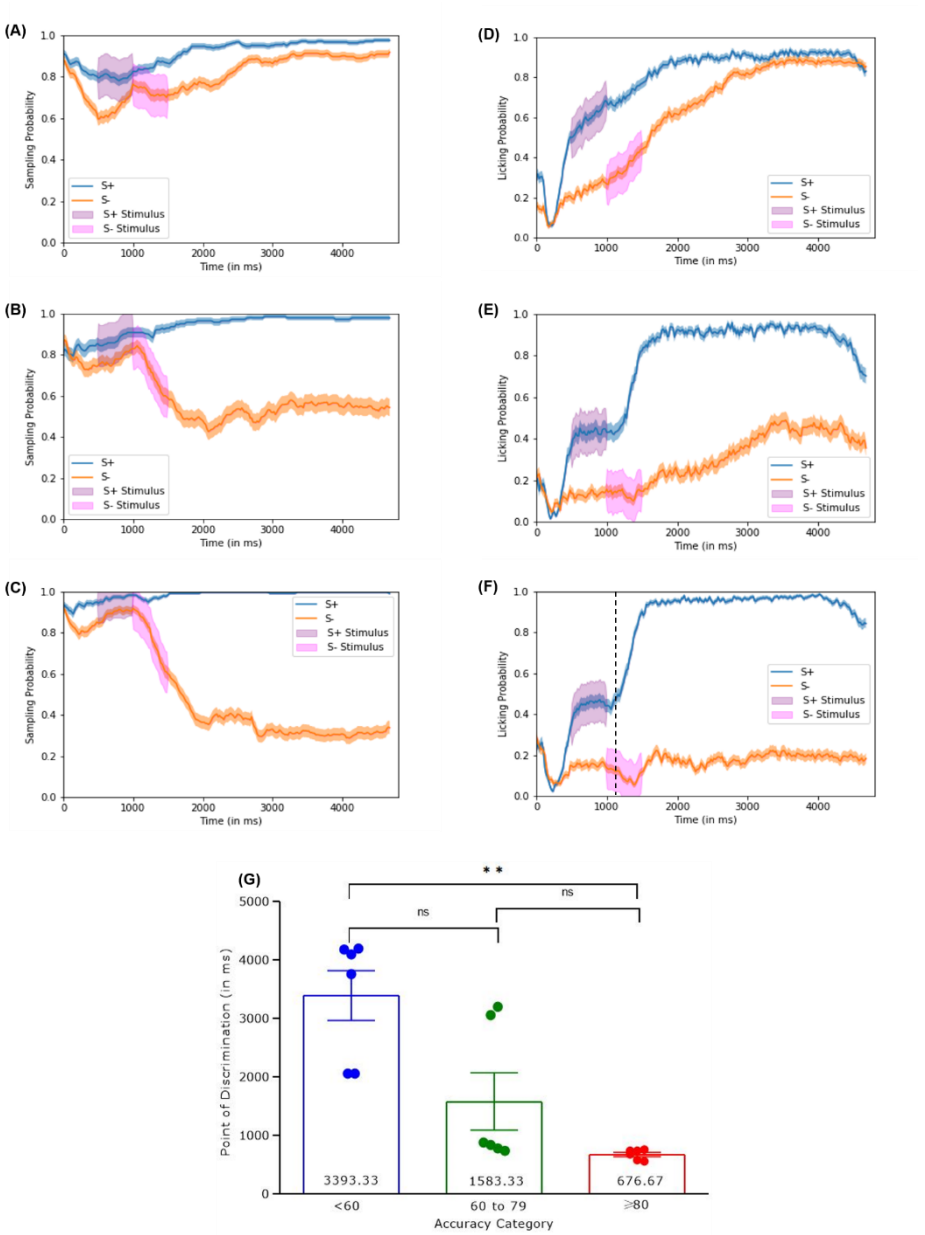

Figure 15: Visualizing evolution of sampling and licking responses of animals which learn to discriminate between temporal delays in odor presentation

(A-C). (A) We see a varying sampling response trace for non-rewarded trials indicating the behavioral uncertainty of the animal when it is naïve and is presented with same odor at different timings; (B) The sampling response for non-rewarded is not inconsistent as in (A), however, the animal requires more learning to discriminate between the nature of trial with better accuracy; (C) As observed in sampling responses for previous experiments, the sampling response for non-rewarded trials rapidly decreases as the animal learns to discriminate between the timings; The width of span representing stimulus delivery window is arbitrarily kept to be 0.1

(D-F). (D) We encounter that initially the animal reduces its licking for the non-rewarded trials, however, during the reaction window it increases again and thus, committing more mistakes. (E) As the animal is learning to distinguish between timings, it elicits a different licking response for rewarded and non-rewarded trials, however, still during the reaction window, the animal shows slight increase in licking for non-rewarded trials; (F) Once the animal learns to properly differentiate between the timings, the licking during reaction window for non-rewarded trials disappears, PoD for this animal represented by black dotted line; The width of span representing stimulus delivery window is arbitrarily kept to be 0.1

(G). The PoD don't show a significant difference between the PoD when the animals are completely naïve and they are learning. Similarly, there is no significant difference while they are learning and have learned with high accuracy. However, if we compare the PoD of the animals when they are completely naïve with that when they have learned the task, we find a drastic decrease in their PoD values (n = 7, RM one-way ANOVA, p=0.0288, F=9.091; Tukey's multiple comparisons test (p<0.2115 for '<60' vs. '60 to 79', p<0.0033 for '<60' vs. '≥80 ', p=0.2548 for '60 to 79' vs.'≥80'))

4.6 Ongoing Experiment

Based on the observation from previous experiments, we concluded that in a population, some animals could learn to discriminate odor timing. Recently, it has been proposed that, the glomeruli which get activated earlier during active sampling, provide the most information about the odor stimulus (Chong et al., 2019). To test for how this proposal would play a role in context of discriminating odor timing, we modified our experimental protocol by reducing the delays accordingly.

We began with the second phase of the experiment, following the protocol as given**.** In the second phase, we have reduced the duration of delays throughout each trial. In the second phase, the rewarded odor is delivered after a delay of 100 ms. Similarly, the non-rewarded stimulus is delivered after 200 ms of delay. Instead of 2500 ms, as in the case of Phase 1, now the total background (room air, no odor) exposure window is 400 ms. This window is followed by a tone of 200 ms and then by the reaction window of 2000 ms. A schematic for the Phase 2 protocol has

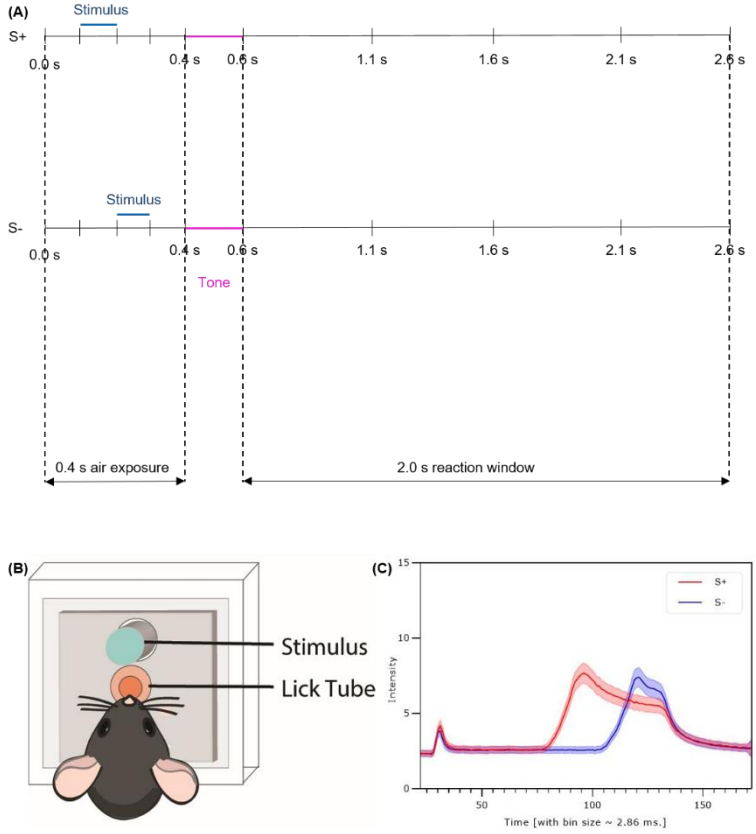

Figure 16: Protocol of Phase 2

(A). Schematic of protocol for Phase 2 experiments

(B). Schematic of delivery system used in Phase 2 experiments

(C). PID signal for Phase 2 protocol exhibiting that the non-rewarded stimulus is delivered at a later timing as compared to the rewarded stimulus

been given below (Figure 16A). A new set (n = 10) was used for this experiment. Unlike in Phase 1, animals were directly subjected to timing discrimination task in Phase 2. Along with that, the delivery system was modified (Figure 16B) to deliver a more focused odor plume. To ensure that the valves were opening at different timings, a PID was used to check for odor signals during stimulus presentation for 40 (20 rewarded and 20 non-rewarded) trials. The mean signal trace with SEM as a spread around the mean signal trace has been given below (Figure 16C).

Animals have completed around 1200 trials. However, we did not observe any learning Figure 17.

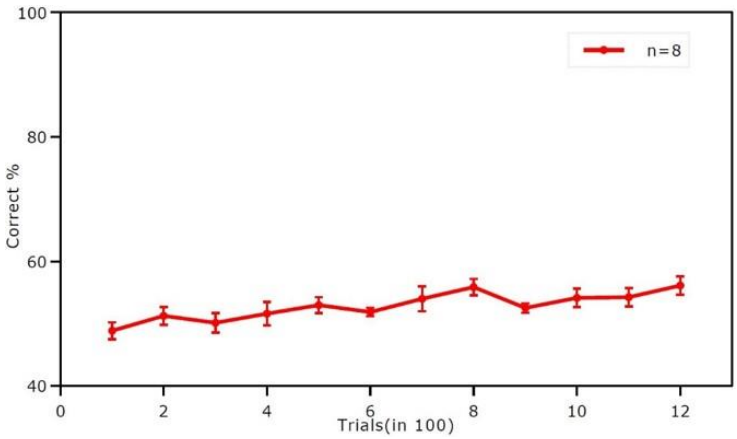

Figure 17: Learning curve for task involving presentation of same target odor at two different delays

5 Discussion

We performed behavioral assays to investigate if rodents can discriminate between different timing of odor presentation. We began by challenging the animals to distinguish between an enantiomer pair, each delivered at two different timings. We then proceeded by gradually increasing the complexity of the task by reducing the dissimilarity of the target odors, eventually delivering the same target odor at two different delays. We observed that animals learned for experiments involving different target odors readily. For the experiment involving a mixture of enantiomers, animals learned the task with high accuracy, albeit only after performing an extra task. Ultimately, when animals were challenged to discriminate between the timing of odor delivery of the same target odor, only seven out of twelve animals could learn.

Throughout the experiments, we have seen that animals make a decision during the time window of non-rewarded stimulus (1000-1500 ms) irrespective of the type of stimulus. In experiments for which animals are being provided with an extra cue of odor difference (other than odor timing), it might be speculated that animals would use the difference between the odor identities as the cue to discriminate between rewarded and non-rewarded trials. If that was the case, we should have seen two different PoDs, for rewarded trials during the 500-1000 ms window, for non-rewarded trials, during the 1000-1500 ms window. What we observe instead (Figure 9, Figure 11, Figure 13, Figure 15), is that the sampling and licking responses for rewarded vs. non-rewarded trials diverge at the same time point, irrespective of the nature of the trial (rewarded or non-rewarded). It implies that they wait for the duration of rewarded stimulus to finish before they respond for any type of stimulus, thus indicating that they can detect temporal cue associated with the odor presentation. However, when we subject them to differentiate between rewarded and non-rewarded trials based only upon the timing of the same target odor presentation for rewarded vs. non-rewarded, we get a variable response. Some of them learn the task. This suggests that rodents can detect temporal delays within odor presentation. However, they use this ability in conjunction with their ability to discriminate between odorants. If challenged to discriminate between timing, using the same target odor, not all of them can learn at an equal pace.

Previous attempts of studying if rodents can discriminate between the timing of virtual odor presentation (optogenetic activation) have been successful, and they did not

report of requiring unusually more number of training sessions (Smear et al., 2011, 2013). In our case, we needed a significantly more number of sessions for the animals to learn discriminating temporal delays. This difference could have arisen as a result of the difference between optogenetic mode of stimulation and natural odor delivery. Using optogenetic stimulation at the glomerular layer gives precise control over stimulus presentation. Thus, the spatiotemporal evolution of glomerular activation pattern remains uniform across trials. However, when we use natural odor stimulation, the sampling behavior of the animal comes into play. It has been shown that animals actively modulate their sniffing behavior during decision making (Bhattacharjee et al., 2019). Thus, animals that are able to learn might be able to do so due to the optimum modulation of their sniffing. However, those animals which are unable to do so might be facing difficulty in discriminating between odor presentation timings. Furthermore, we have considered the static spatial patterns of odors for target vs. the background on the dorsal surface of the olfactory bulb. Amyl acetate, which serves as our background odor, has a broad spatiotemporal activity pattern. Thus, if our target odor spatiotemporal profile would have coinciding glomerular activation patterns as that of the background, then that might make it difficult for the animals to discriminate between the relative timing of glomerular pattern activation. Also, the animals who were unable to learn the timing discrimination task had performed with high accuracy for all the previous experiments. This learning deficit illustrates the subjective difference between the learning abilities of individual animals.

Recently, researchers proposed an idea of ‘primacy coding’ to explain odor coding in the OB. It states that, the glomeruli which get activated earlier during active sampling, provide the most information about odor stimulus (Chong et al., 2019). To investigate if the above hypothesis is applicable in context of coding delays, we introduced another training scheme by reducing delays involved throughout each trial (Phase 2). However, as the learning curve in the “Results-Ongoing work” section depicts, there is no learning even after the animals have been trained for more than 1200 trials (ongoing work).

Lastly, it has been shown that segregating relevant odor against the background is strongly dependent on the extent of overlap between the glomerular pattern elicited by the target and the background odors (Rokni et al., 2014). In our case, we have used a single background odor (Amyl acetate), which elicits a broad glomerular pattern.

Additionally, we supply a continuous stream of background to the animals. These two factors might mask the contribution of newly activated glomeruli due to the target presentation, thus reducing their contribution to forming the odor identity of the target odor. Hence, the contrast between background vs. target wouldn't fully manifest itself, which might lead to reduced learning pace and the learning deficit observed in some animals. Under such a case, the sampling strategies of animals could help compensate by providing the necessary amount of temporal discontinuity for the segregation of glomerular patterns for the target vs. background. This would also, explain the subjectivity involved in the learning phenotype, as not all animals would find the perfect sampling strategy at an equal pace. However, under natural settings, all the odors (target and background) vary on shorter timescales. Thus, there is a continual change in the patterns elicited at the glomerular layer by all odors. This temporal change in glomerular patterns might assist in enhancing the contrast between the target vs. background odor. To test this possibility, we would need to present multiple odors while having a precise temporal control over the application of each odor. Our freely moving setup limits us from designing an experiment to investigate the above hypothesis. However, using a head-restrained set-up, we can present multiple odors simultaneously in the form of plumes, and then use one of them as a target odor while others can serve as a background. Then, by associating this odor with two different time points of the presentation, we could discern if animals can detect temporal delays in their natural environments, and if the fluctuating odor plumes in nature serve beneficial for target vs. background segregation.

6 Bibliography

Abraham, N. M., Egger, V., Shimshek, D. R., Renden, R., Fukunaga, I., Sprengel, R., Seeburg, P. H., Klugmann, M., Margrie, T. W., & Schaefer, A. T. (2010). Synaptic inhibition in the olfactory bulb accelerates odor discrimination in mice. *Neuron*, *65*(3), 399–411.

Abraham, N. M., Spors, H., Carleton, A., Margrie, T. W., Kuner, T., & Schaefer, A. T. (2004). Maintaining accuracy at the expense of speed: Stimulus similarity defines odor discrimination time in mice. *Neuron*, *44*(5), 865–876.

Baker, K. L., Vasan, G., Gumaste, A., Pieribone, V. A., & Verhagen, J. V. (2019). Spatiotemporal dynamics of odor responses in the lateral and dorsal olfactory bulb. *PLoS Biology*, *17*(9), e3000409.

Bhattacharjee, A. S., Konakamchi, S., Turaev, D., Vincis, R., Nunes, D., Dingankar, A. A., Spors, H., Carleton, A., Kuner, T., & Abraham, N. M. (2019). Similarity and Strength of Glomerular Odor Representations Define a Neural Metric of Sniff-Invariant Discrimination Time. *Cell Reports*, *28*(11), 2966–2978.

Cenier, T., Amat, C., Litaudon, P., Garcia, S., Lafaye de Micheaux, P., Liquet, B., Roux, S., & Buonviso, N. (2008). Odor vapor pressure and quality modulate local field potential oscillatory patterns in the olfactory bulb of the anesthetized rat. *European Journal of Neuroscience*, *27*(6), 1432–1440.

Chong, E., Moroni, M., Wilson, C., Shoham, S., Panzeri, S., & Rinberg, D. (2019). Manipulating synthetic optogenetic odors reveals the coding logic of olfactory perception. *BioRxiv*, 841916.

Cleland, T. A., & Linster, C. (1999). Concentration tuning mediated by spare receptor capacity in olfactory sensory neurons: A theoretical study. *Neural Computation*, *11*(7), 1673–1690.

Davison, I. G., & Ehlers, M. D. (2011). Neural circuit mechanisms for pattern detection and feature combination in olfactory cortex. *Neuron*, *70*(1), 82–94.

Doty, R. L. (1986). Odor-guided behavior in mammals. *Experientia*, *42*(3), 257–271.

Eaton, B. E., Gold, L., & Zichi, D. A. (1995). Let's get specific: The relationship between specificity and affinity. *Chemistry & Biology*, *2*(10), 633–638.

Erskine, A., Ackels, T., Dasgupta, D., Fukunaga, I., & Schaefer, A. T. (2019). Mammalian olfaction is a high temporal bandwidth sense. *BioRxiv*, 570689.

Firestein, STUART, Picco, C., & Menini, A. (1993). The relation between stimulus and response in olfactory receptor cells of the tiger salamander. *The Journal of Physiology*, *468*(1), 1–10.

Firestein, Stuart, & Shepherd, G. M. (1991). A kinetic model of the odor response in single olfactory receptor neurons. *The Journal of Steroid Biochemistry and Molecular Biology*, *39*(4), 615–620.

Frasnelli, J., Wohlgemuth, C., & Hummel, T. (2006). The influence of stimulus duration on odor perception. *International Journal of Psychophysiology*, *62*(1), 24–29.

Fukunaga, I., Berning, M., Kollo, M., Schmaltz, A., & Schaefer, A. T. (2012). Two distinct channels of olfactory bulb output. *Neuron*, *75*(2), 320–329.

Hayar, A., Karnup, S., Ennis, M., & Shipley, M. T. (2004). External tufted cells: A major excitatory element that coordinates glomerular activity. *Journal of Neuroscience*, *24*(30), 6676–6685.

Hayar, A., Karnup, S., Shipley, M. T., & Ennis, M. (2004). Olfactory bulb glomeruli: External tufted cells intrinsically burst at theta frequency and are entrained by patterned olfactory input. *Journal of Neuroscience*, *24*(5), 1190–1199.

Howard, W. E., Marsh, R. E., & Cole, R. E. (1968). Food detection by deer mice using olfactory rather than visual cues. *Animal Behaviour*.

Isaacson, J. S., & Strowbridge, B. W. (1998). Olfactory Reciprocal Synapses: Dendritic Signaling in the CNS. *Neuron*, *20*(4), 749–761. https://doi.org/10.1016/S0896-6273(00)81013-2

Jacobs, G. H., Fenwick, J. A., & Williams, G. A. (2001). Cone-based vision of rats for ultraviolet and visible lights. *Journal of Experimental Biology*, *204*(14), 2439–2446.

Ko, H. J., Lee, S. H., Oh, E. H., & Park, T. H. (2010). Specificity of odorant-binding proteins: A factor influencing the sensitivity of olfactory receptor-based biosensors. *Bioprocess and Biosystems Engineering*, *33*(1), 55.

Kosaka, K., Toida, K., Aika, Y., & Kosaka, T. (1998). How simple is the organization of the olfactory glomerulus?: The heterogeneity of so-called periglomerular cells. *Neuroscience Research*, *30*(2), 101–110.

Lancet, D. (1986). Vertebrate olfactory reception. *Annual Review of Neuroscience*, *9*(1), 329–355.

Li, A., Gire, D. H., Bozza, T., & Restrepo, D. (2014). Precise detection of direct glomerular input duration by the olfactory bulb. *Journal of Neuroscience*, *34*(48), 16058–16064.

Linster, C., Johnson, B. A., Yue, E., Morse, A., Xu, Z., Hingco, E. E., Choi, Y., Choi, M., Messiha, A., & Leon, M. (2001). Perceptual correlates of neural representations evoked by odorant enantiomers. *Journal of Neuroscience*, *21*(24), 9837–9843.

Macrides, F., & Schneider, S. P. (1982). Laminar organization of mitral and tufted cells in the main olfactory bulb of the adult hamster. *Journal of Comparative Neurology*, *208*(4), 419–430.

Margrie, T. W., Sakmann, B., & Urban, N. N. (2001). Action potential propagation in mitral cell lateral dendrites is decremental and controls recurrent and lateral inhibition in the mammalian olfactory bulb. *Proceedings of the National Academy of Sciences*, *98*(1), 319–324.

Mitchell, L., Cheney, K. L., Cortesi, F., Marshall, N. J., & Vorobyev, M. (2017). Triggerfish uses chromaticity and lightness for object segregation. *Royal Society Open Science*, *4*(12), 171440.

Miura, K., Mainen, Z. F., & Uchida, N. (2012). Odor representations in olfactory cortex: Distributed rate coding and decorrelated population activity. *Neuron*, *74*(6), 1087–1098.

Miyamichi, K., Amat, F., Moussavi, F., Wang, C., Wickersham, I., Wall, N. R., Taniguchi, H., Tasic, B., Huang, Z. J., & He, Z. (2011). Cortical representations of olfactory input by trans-synaptic tracing. *Nature*, *472*(7342), 191–196.

Mombaerts, P. (1999). Molecular biology of odorant receptors in vertebrates. *Annual Review of Neuroscience*, *22*(1), 487–509.

Mombaerts, P., Wang, F., Dulac, C., Chao, S. K., Nemes, A., Mendelsohn, M., Edmondson, J., & Axel, R. (1996). Visualizing an olfactory sensory map. *Cell*, *87*(4), 675–686.

Mouse Genome Sequencing Consortium, Waterston, R. H., Lindblad-Toh, K., Birney, E., Rogers, J., Abril, J. F., Agarwal, P., Agarwala, R., Ainscough, R., Alexandersson, M., An, P., Antonarakis, S. E., Attwood, J., Baertsch, R., Bailey, J., Barlow, K., Beck, S., Berry, E., Birren, B., … Lander, E. S. (2002). Initial sequencing and comparative analysis of the mouse genome. *Nature*, *420*(6915), 520–562. https://doi.org/10.1038/nature01262

Nagayama, S., Homma, R., & Imamura, F. (2014). Neuronal organization of olfactory bulb circuits. *Frontiers in Neural Circuits*, *8*, 98.

Parabucki, A., Bizer, A., Morris, G., Munoz, A. E., Bala, A. D., Smear, M., & Shusterman, R. (2019). Odor concentration change coding in the olfactory bulb. *Eneuro*, *6*(1).

Perl, O., Nahum, N., Belelovsky, K., & Haddad, R. (2020). The contribution of temporal coding to odor coding and odor perception in humans. *ELife*, *9*.

Pinching, A. J., & Powell, T. P. S. (1971). The neuron types of the glomerular layer of the olfactory bulb. *Journal of Cell Science*, *9*(2), 305–345.

Price, J. L. J. (2009). Olfactory higher centers anatomy. In *Encyclopedia of neuroscience* (pp. 129–136). Elsevier Ltd.

Rebello, M. R., McTavish, T. S., Willhite, D. C., Short, S. M., Shepherd, G. M., & Verhagen, J. V. (2014). Perception of odors linked to precise timing in the olfactory system. *PLoS Biology*, *12*(12), e1002021.

Resulaj, A., & Rinberg, D. (2015). Novel behavioral paradigm reveals lower temporal limits on mouse olfactory decisions. *Journal of Neuroscience*, *35*(33), 11667–11673.

Rokni, D., Hemmelder, V., Kapoor, V., & Murthy, V. N. (2014). An olfactory cocktail party: Figure-ground segregation of odorants in rodents. *Nature Neuroscience*, *17*(9), 1225.

Roux, F.-E., Djidjeli, I., & Durand, J.-B. (2018). Functional architecture of the somatosensory homunculus detected by electrostimulation. *The Journal of Physiology*, *596*(5), 941–956.

Rubin, B. D., & Katz, L. C. (2001). Spatial coding of enantiomers in the rat olfactory bulb. *Nature Neuroscience*, *4*(4), 355–356.

Sato, T., Homma, R., & Nagayama, S. (2020). Direct Comparison of Odor Responses of Homologous Glomeruli in the Medial and Lateral Maps of the Mouse Olfactory Bulb. *Eneuro*, *7*(2), ENEURO.0449-19.2020. https://doi.org/10.1523/ENEURO.0449-19.2020

Shepherd, G. M., & Greer, C. A. (1998). Olfactory bulb. In *The Synaptic Organization of the Brain* (GM Shepherd, pp. 159–203). New York: Oxford Univ. Press.

Slotnick, B., & Restrepo, D. (2005). Olfactometry with mice. *Current Protocols in Neuroscience*, *33*(1), 8–20.

Smear, M., Resulaj, A., Zhang, J., Bozza, T., & Rinberg, D. (2013). Multiple perceptible signals from a single olfactory glomerulus. *Nature Neuroscience*, *16*(11), 1687.

Spors, H., & Grinvald, A. (2002). Spatio-temporal dynamics of odor representations in the mammalian olfactory bulb. *Neuron*, *34*(2), 301–315.

Spors, H., Wachowiak, M., Cohen, L. B., & Friedrich, R. W. (2006). Temporal dynamics and latency patterns of receptor neuron input to the olfactory bulb. *Journal of Neuroscience*, *26*(4), 1247–1259.

Stern, M., Bolding, K. A., Abbott, L. F., & Franks, K. M. (2018). A transformation from temporal to ensemble coding in a model of piriform cortex. *Elife*, *7*, e34831.

Stettler, D. D., & Axel, R. (2009). Representations of odor in the piriform cortex. *Neuron*, *63*(6), 854–864.

Vassar, R., Ngai, J., & Axel, R. (1993). Spatial segregation of odorant receptor expression in the mammalian olfactory epithelium. *Cell*, *74*(2), 309–318.

Yokoi, M., Mori, K., & Nakanishi, S. (1995). Refinement of odor molecule tuning by dendrodendritic synaptic inhibition in the olfactory bulb. *Proceedings of the National Academy of Sciences*, *92*(8), 3371–3375.

Zapiec, B., & Mombaerts, P. (2020). The Zonal Organization of Odorant Receptor Gene Choice in the Main Olfactory Epithelium of the Mouse. *Cell Reports*, *30*(12), 4220–4234.